Advances in Colloid and Interface Science 350 (2026) 103775

Contents lists available at ScienceDirect

Advances in Colloid and Interface Science

journal homepage: www.elsevier.com/locate/cis

Antimicrobial peptides at (lipid) interfaces: Insights from monolayer models

Paula Antelo-Riveiro [a,b], Rebeca Garcia-Fandino [a,*], Ángel Piñeiro [b,*]

[a] Department of Organic Chemistry, Center for Research in Biological Chemistry and Molecular Materials, Santiago de Compostela University, CIQUS, Spain
[b] Department of Applied Physics, Faculty of Physics, University of Santiago de Compostela, Spain

ARTICLE INFO

Keywords:
Antimicrobial peptides
Lipid interfaces
Peptide-lipid interactions
Interfacial thermodynamics
Langmuir monolayers
Molecular modeling

ABSTRACT

Antimicrobial peptides (AMPs) are key effectors of innate immunity that, beyond their canonical activity, exhibit promising therapeutic potential against cancer and cellular senescence. Their efficacy relies on selective membrane disruption driven by specific lipid signatures, yet quantifying these interactions in complex bilayer systems remains challenging. Lipid monolayers serve as powerful reductionist models to isolate the physicochemical determinants of this selectivity, effectively mimicking the outer leaflet of bacterial, cancerous, or senescent membranes. This review provides a critical analysis of how lipid composition, packing density, and phase behavior modulate AMP adsorption and insertion. We systematically integrate thermodynamic profiling (surface pressure, compressibility, mixing energy) with advanced structural and morphological characterization. Special emphasis is placed on how spectroscopic techniques (IRRAS, GIXD, SFG) and real-time microscopy (BAM, fluorescence, AFM) resolve peptide orientation, secondary structure induction, and lipid domain remodeling at the mesoscale. These experimental observables are bridged with Molecular Dynamics (MD) simulations, establishing a feedback loop between macroscopic measurements and atomistic resolution. By defining the advantages and limitations of monolayer models relative to vesicles and bilayers, we outline a rational framework for leveraging interfacial insights in the design of next-generation peptide therapeutics and nanobiotechnological applications.

1. Introduction

AMPs constitute evolutionarily conserved effectors of innate immunity [1]. Unlike conventional antibiotics that target intracellular machinery, the biological antimicrobial activity (BAA) of AMPs is primarily driven by direct physicochemical interactions with cellular membranes [2,3]. This lipid-targeting mechanism confers rapid bactericidal action and reduces susceptibility to resistance development, positioning AMPs as critical tools in the fight against antimicrobial resistance (AMR) [4,5]. However, deciphering the thermodynamic principles that translate interfacial surface activity (ISA) into biological efficacy remains a fundamental challenge [6].

Beyond infectious diseases, AMPs participate in diverse physiological and pathological processes involving membrane remodeling, including cancer cell targeting [7–9], immune modulation, chronic inflammation [10,11], neuronal regulation [12], and tissue regeneration [13,14]. This therapeutic versatility relies on the peptide's ability to exploit compositional differences between microbial, cancerous, and

Abbreviation: AA-MD, All-Atom Molecular Dynamics; aMD, Accelerated Molecular Dynamics; AFM, Atomic Force Microscopy; AMP, Antimicrobial Peptide; AMR, Antimicrobial Resistance; AI, Artificial Intelligence; BAA, Biological Antimicrobial Activity; BAM, Brewster Angle Microscopy; BLM, Black Lipid Membrane; CD, Circular Dichroism; CG-MD, Coarse-Grained Molecular Dynamics; CMC, Critical Micelle Concentration; DPPC, Dipalmitoylphosphatidylcholine; DPPG, Dipalmitoylphosphatidylglycerol; EoS, Equation of State; FCS, Fluorescence Correlation Spectroscopy; GIXD, Grazing Incidence X-ray Diffraction; GUV, Giant Unilamellar Vesicle; HT-MD, High-Temperature Molecular Dynamics; IRRAS, Infrared Reflection-Absorption Spectroscopy; ISA, Interfacial Surface Activity; Lα, Liquid-crystalline (fluid) phase; Lβ, Gel phase; LC, Liquid-Condensed (phase); LE, Liquid-Expanded (phase); Lo, Liquid-ordered (phase); LUV, Large Unilamellar Vesicle; MD, Molecular Dynamics; MSD, Mean Square Displacement; NR, Neutron Reflectometry; PC, Phosphatidylcholine; PE, Phosphatidylethanolamine; PG, Phosphatidylglycerol; PS, Phosphatidylserine; REMD, Replica Exchange Molecular Dynamics; SAM, Self assembled monolayer; SeoS, Surface equation of state; SFG, Sum Frequency Generation; SLB, Supported Lipid Bilayer; SM, Sphingomyelin; SUV, Small Unilamellar Vesicle; TEM, Transmission Electron Microscopy; TRIC, Trichogin GA IV; XR / XRR, X-ray Reflectivity; π–A, Surface Pressure–Area.

* Corresponding authors.
E-mail addresses: rebeca.garcia.fandino@usc.es (R. Garcia-Fandino), angel.pineiro@usc.es (Á. Piñeiro).

https://doi.org/10.1016/j.cis.2025.103775
Received in revised form 30 December 2025;
Available online 2 January 2026

healthy cells [12,15]. Such selectivity arises from specific structural features including lipid charge, packing density, and acyl-chain chemistry [16–23]. For instance, bacterial membranes are enriched in anionic phospholipids such as PG [18], promoting electrostatic attraction to cationic residues, whereas mammalian membranes predominantly display zwitterionic species [19]. Pathological conditions, including cancer or cellular senescence, may externalize PS or alter packing [20,21], thereby increasing susceptibility to AMP binding and disruption. Functionally, AMPs operate through multiple membrane-active mechanisms, including adsorption, carpet-like disruption, pore formation (barrel-stave or toroidal models), lipid clustering, electroporation, and non-lytic depolarization (Fig. 1) [22].

Biological membranes themselves are complex, heterogeneous bilayers composed of proteins, carbohydrates, and cholesterol, exhibiting variable headgroup chemistry, curvature, and lateral organization [23]. These properties tune membrane fluidity, surface potential, and susceptibility to AMP-induced perturbation. To dissect these interactions, a range of model systems have been developed, including small, large and giant unilamellar lipid vesicles (SUVs, LUVs, GUVs) and supported lipid bilayers (SLBs) [24–26]. These models enable the visualization of large-scale morphological responses, membrane thinning, and bilayer-coupled processes under hydrated conditions. However, because bilayers inherently couple their leaflets and respond globally to deformation, they complicate mechanistic isolation of interfacial parameters such as lateral pressure, leaflet composition, and packing elasticity [24–26]. Lipid monolayers at the air–water interface provide a complementary and reductionist model that isolates outer-leaflet phenomena. Their planar geometry enables precise control over composition, packing density, and surface pressure [27], and they serve as structurally and thermodynamically relevant approximations of cellular outer leaflets. Classical studies showed that monolayers induce secondary structure in peptides otherwise disordered in solution, particularly α-helices [28,29]. Their capacity to quantify insertion depth, lateral organization, domain formation, and packing-dependent conformational transitions has also been shown [30]. Furthermore, techniques such as Infrared Reflection–Absorption Spectroscopy (IRRAS) allow in situ determination of peptide conformation and orientation without perturbing the film [31,32].

While monolayers offer unparalleled resolution of interfacial determinants of AMP function, their translation to biological membranes requires caution. They lack features such as leaflet coupling, curvature, hydration gradients, and transmembrane pore formation pathways, which are central to downstream antimicrobial events. Moreover, interpretations across monolayers, vesicles, and bilayers are not always consistent, and open questions persist regarding how interfacial packing, leaflet asymmetry, and lateral pressure propagate across membrane architectures [30,33] and how interfacial insights relate to BAA outcomes [24–27,33].

This review integrates biophysical mechanisms, interfacial models, and characterization strategies to provide a coherent framework linking the physicochemical behavior of AMPs at the air–water interface with their biological membrane-disruptive activity. Experimental and computational approaches—ranging from Langmuir-based thermodynamic measurements to spectroscopy, microscopy, interfacial rheology, and molecular simulations—are critically examined to explain how they provide complementary and sometimes orthogonal observables that enable a mechanistic interpretation of AMP–monolayer interactions. This integrated perspective positions monolayers as quantitative, hypothesis-driven model systems that bridge simplified interfacial studies with the complex biological behavior of AMPs.

2. Key structural and functional properties of antimicrobial peptides

AMPs are characterized by distinctive molecular properties that enable selective interactions with microbial membranes while

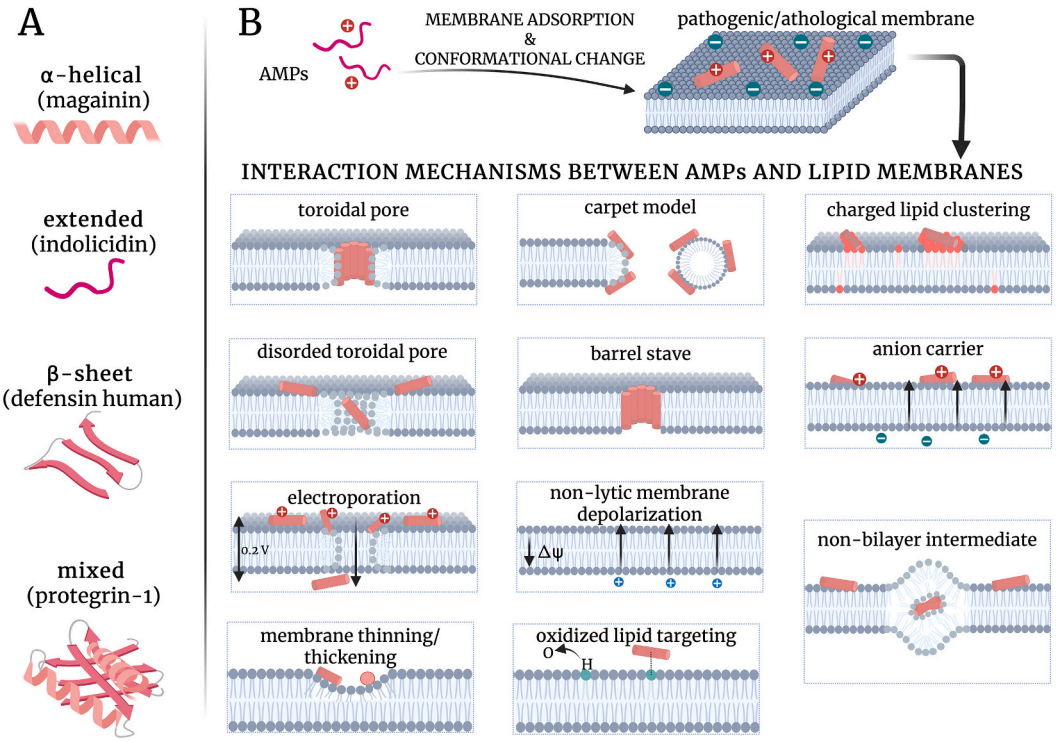

Fig. 1. Structural diversity of AMPs and their membrane-disrupting mechanisms. (A) AMPs adopt diverse structural motifs, including α-helices (magainin), extended structures (indolicidin), β-sheets (human defensin), and mixed conformations (protegrin-1), which influence their mode of action. (B) AMPs interact with bacterial membranes through various mechanisms, including membrane adsorption, pore formation (barrel stave, toroidal pore), the carpet model, electroporation, lipid clustering, and non-lytic depolarization.

minimizing toxicity toward host cells. These features—including amphiphilicity and cationic charge typically involving 40–60 % of hydrophobic residues, as well as structural motifs like α-helices and β-sheets (Fig. 2)—are not only critical to their antimicrobial efficacy but also play integral roles in driving interfacial assembly and ISA within monolayer systems [28].

Many AMPs are intrinsically disordered in aqueous environments but undergo conformational transitions upon membrane contact, adopting ordered structures that optimize their ISA and eventually their BAA. This structural plasticity enables AMPs to respond dynamically to changes in lipid composition and interfacial conditions, facilitating insertion, alignment, and membrane destabilization. Alamethicin and magainin 2 are examples of AMPs that remain largely unstructured in solution but adopt well-defined amphipathic α-helices upon interaction with lipid monolayers [29–32]. This conformational transition promotes insertion into the interface and disrupts lipid packing, linking secondary structure formation directly to membrane perturbation. Their dual hydrophobic and hydrophilic character promotes alignment parallel to the interface, enabling deep insertion and lateral organization within the membrane. These properties have made them prototypical models for helix-driven membrane interactions and valuable tools for studying AMP behavior in monolayer systems. Similar behavior is observed in LL-37, a human cathelicidin that forms an amphipathic α-helix aligned parallel to lipid interfaces [34,35]. This conformation enhances both hydrophobic insertion and electrostatic anchoring, leading to disruption of lipid organization and increased membrane fluidity. In contrast, its truncated fragment LL-20—lacking key structural regions—fails to adopt ordered structures at the interface, resulting in diminished antimicrobial potency [36]. Other β-sheet-forming peptides such as arenicins and defensins tend to lie flat at the interface, maximizing surface contact and promoting membrane destabilization through extended intermolecular interactions [37,38]. β-sheet lipopeptides also exhibit this behavior, forming stable, well-ordered monolayers that enhance interfacial disruption through their extended lateral packing [39].

In addition to amphiphilicity and structural adaptability, a high net positive charge—typically conferred by lysine and arginine residues—is critical for strong electrostatic interactions with negatively charged bacterial membranes. These interactions are particularly relevant for membranes enriched in anionic phospholipids, such as phosphatidylglycerol (PG), cardiolipin (CL), or externalized phosphatidylserine (PS), which are commonly found not only in bacteria but also in cancer cells, senescent cells, and other pathophysiological states. In contrast, zwitterionic lipids like phosphatidylcholine (PC), predominant in mammalian membranes, exhibit reduced affinity for AMPs [40]. Charge density determines not only the binding affinity of AMPs to anionic phospholipids such as dipalmitoylphosphatidylglycerol (DPPG) but also the depth of peptide penetration into monolayers. For example, protegrin-1 (PG-1) demonstrates selective adsorption and destabilization of bacterial lipid monolayers such as DPPG, while sparing mammalian dipalmitoylphosphatidylcholine (DPPC) monolayers [41,42]. LL-37, an intrinsically disordered AMP in aqueous solution, adopts an α-helical conformation upon binding to anionic lipid interfaces, which enables efficient monolayer disruption at low peptide-to-lipid ratios due to its high charge density [34,35]. However, at elevated surface concentrations, excessive charge can lead to interfacial crowding, peptide accumulation at domain boundaries, or even partial exclusion from the monolayer, as observed in Langmuir films containing highly charged peptide–lipid mixtures [43]. These effects may hinder optimal insertion and reduce the overall efficiency of membrane perturbation.

Hydrophobic interactions also play a central role by promoting deeper peptide insertion and anchoring within the membrane core. These interactions, involving the hydrophobic faces of amphipathic helices or the β-sheet surface, drive membrane thinning, lipid reorganization, and pore formation [44–46]. Modifying hydrophobic content—such as through leucine substitutions—has been shown to enhance penetration and lipid packing disruption, while maintaining selectivity for bacterial over mammalian membranes [43,47].

To better understand and categorize AMPs based on their structural and functional characteristics, several dedicated databases provide comprehensive information on sequence diversity, antimicrobial activity, and biophysical properties [48,49] (see Table 1). The scale of this diversity is reflected in current repositories; for instance, the APD6 database contains 5680 curated natural and synthetic peptides [53,54], while platforms like ADAPTABLE have unified over 40,000 sequences to facilitate property-alignment studies [60]. These resources facilitate the systematic classification of AMPs, enabling researchers to correlate specific physicochemical properties with their interactions at lipid monolayers, guiding their experimental validation and providing valuable insights for the design of novel therapeutic peptides and biotechnological applications. Indeed, the use of deep learning algorithms for peptide design is an ongoing and promising field of research today [50–52].

3. Lipid composition and biomimetic models for understanding antimicrobial peptide-membrane interactions

Biological membranes are complex and dynamic structures in which lipids constitute the main structural and functional components [23,67].

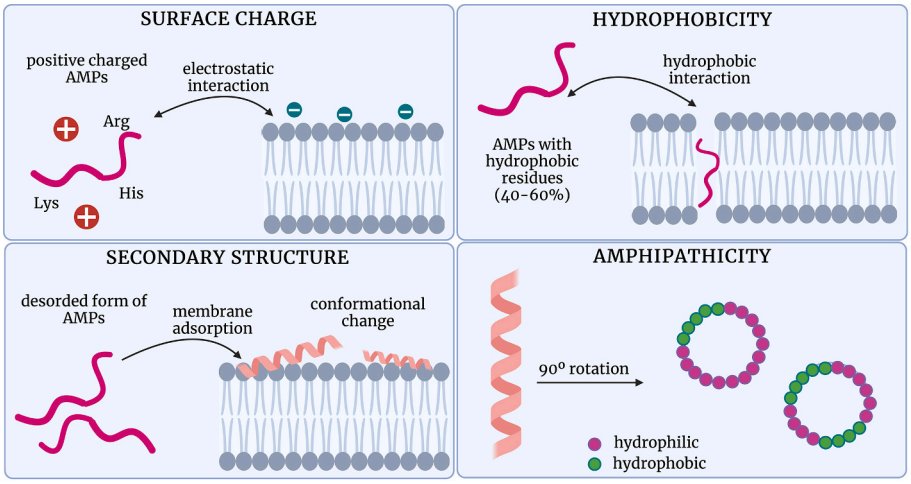

Fig. 2. Key physicochemical properties of antimicrobial peptides governing interactions with lipid bilayers. AMP binding and membrane activity are driven by surface charge, hydrophobicity, secondary structure transitions upon membrane contact, and amphipathic organization. These features collectively determine peptide insertion, alignment, and lipid perturbation in biological membranes.

Table 1
Overview of major AMP databases. The table compares major AMP-focused databases of 2025, including only repositories dedicated to antimicrobial activity. Status refers to current maintenance and web accessibility (A = active; I = inactive). Entry counts correspond to the latest reported version and may not reflect non-redundant integration across sources. URLs include last known access points; offline databases are retained for archival relevance.

DB Name	Status 2025	Entries	Last Update	Focus / Scope	Access / Tools	URL / Reference	Notes
APD6	A	5680	2025	Natural & synthetic curated AMPs	Search + analysis tools, partial downloads	https://aps.unmc.edu/ [53,54]	Validated data; no full bulk download
DRAMP 4.0	A	30,260	2024	Clinical, patent & stability data	Bulk downloads, sequence & activity search	http://dramp.cpu-bioinfor.org/ [55]	Best for translational/ clinical pipeline
CAMPR4	A	24,243	2023	Natural + synthetic; motifs, patents	ML prediction tools, structure search	https://camp.bicnirrh.res.in/ [56]	Uses different predictors for synthetic vs natural
dbAMP 3.0	A	33,065	2024	Genomic & proteomic mining; structural predictions	Download, deep-learning structure tools	https://awi.cuhk.edu.cn/dbAMP/tutorial.php http://bioinformatics.hitsz.edu.cn/dbAMP/home/ [57]	Strong for AMP discovery from omics
DBAASP v3	A	~23,944	2022	Structure–activity & cytotoxicity	API, MD trajectories	https://dbaasp.org/ [58]	Rich structural + MD data
B-AMP v2.0	A	5766	2022	Anti-biofilm & protein targets	Docking pipeline + models	https://b-amp.karishmakaushiklab.com/ [59]	Specialized in biofilms (mechanistic)
ADAPTABLE	A	>40,000	2019	Comprehensive AMP-platform (merged sources, property-alignment)	Search + family generation tools	http://gec.u-picardie.fr/adaptable/ [60]	Unified >40 k sequences; integrates many other AMP datasets
BaAMPs	A	575	2017	Experimental anti-biofilm AMPs	Web search	https://www.baamps.it/ [61]	Specialized in microbial biofilms
LAMP2	I	23,253	2020	Aggregated AMP dataset	Web search	http://biotechlab.fudan.edu.cn/database/lamp [62]	High validation
YADAMP	I	2133	2012	Bacterial AMPs; SAR queries	Site offline	http://www.yadamp.unisa.it/ [63]	Historical SAR resource
ANTIMIC	I	~1700	2004	Sequences + HMM profiling	Site offline	http://research.i2r.a-star.edu.sg/Templar/DB/ANTIMIC/ [64]	Early AMP resource
AMPer	I	1045 + 253	2007	HMM-based AMP classification	Site offline	http://www.cnbi2.com/cgi-bin/amp.pl [65]	Pioneer of automated discovery
RAPD	I	179	2008	Recombinant expression strategies	Site offline	http://faculty.ist.unomaha.edu/chen/rapd/index.php [66]	Number uncertain; data inaccessible

Their molecular diversity—including phospholipids, sterols, and sphingolipids—confers essential properties such as fluidity, lateral packing, surface charge, and phase behavior. These physicochemical parameters critically modulate the interaction of AMPs with membranes, influencing their binding affinity, insertion depth, and disruptive potential. Understanding how specific lipid species contribute to membrane organization and reactivity is therefore fundamental for elucidating AMP mechanisms and guiding their therapeutic optimization. To support this, lipidomic databases such as SwissLipids [68] and Lipid Maps [69], provide detailed information on lipid structures, classifications, and distributions across organisms and tissues. These resources enable the rational design of model membrane systems—such as Langmuir monolayers, vesicles, or supported bilayers—that capture the compositional and biophysical complexity of biological membranes, offering controlled platforms to investigate AMP–lipid interactions.

Phospholipids, the most abundant membrane components, consist of a hydrophilic headgroup and hydrophobic fatty acid tails. The headgroup chemistry determines the membrane's surface charge and governs its electrostatic interactions with peptides, while the acyl chains control membrane fluidity and packing density. In bacterial membranes, anionic phospholipids such as PG and CL provide a negatively charged surface that promotes electrostatic attraction with cationic AMPs, facilitating their selective targeting [18]. In contrast, mammalian cell membranes predominantly contain zwitterionic phospholipids such as PC and sphingomyelin (SM), contributing to a neutral surface charge that reduces AMP affinity and potential cytotoxicity [70]. Cholesterol, a major sterol component in eukaryotic membranes, modulates fluidity and permeability by promoting lipid packing [71] and minimizing AMP-induced disruption.

The lipid composition of mammalian membranes is not static and can change significantly under pathological conditions such as cancer, aging, and chronic inflammation [12]. These conditions often lead to alterations in membrane asymmetry, lipid saturation levels, and overall charge distribution. For instance, in many diseased states, anionic lipids such as PS, which are normally restricted to the inner leaflet of healthy cells, become externalized to the outer leaflet [21]. This altered lipid distribution enhances the susceptibility of such cells to AMP interactions by increasing the electrostatic attraction with cationic peptides (Fig. 3C). Additionally, changes in lipid metabolism associated with

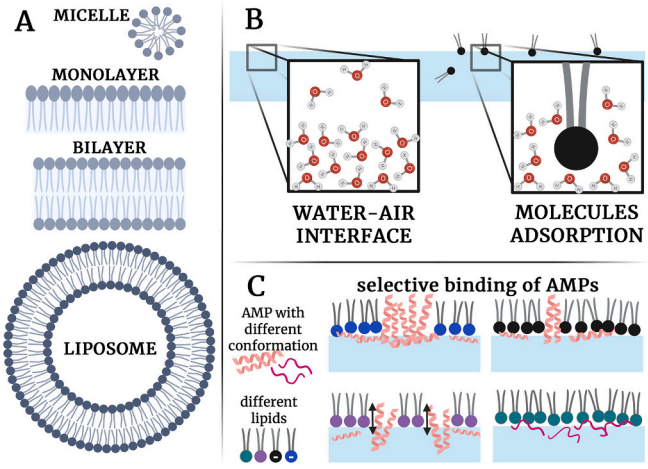

Fig. 3. (A) Model membrane systems. (B) Diagram of a water-air interface and molecules adsorption. (C) Scheme of selective AMP-lipids interactions: the same peptide might interact differently with a variety of lipids, which might lead to the formation of pores, a certain degree of penetration into the monolayer or the absence of a conformational change in the case of weak interaction.

aging and inflammation often result in increased membrane fluidity and altered lipid domain organization, making the membranes more prone to disruption by AMPs [72]. The enrichment of glycosphingolipids and gangliosides in the membranes of cancerous and senescent cells further contributes to the modification of membrane biophysical properties, affecting AMP selectivity and efficacy [73,74].

Beyond headgroup charge, the degree of saturation in the phospholipid acyl chains is a critical determinant of membrane fluidity and packing density, directly influencing AMP insertion. Saturated lipids (e.g., DPPC) tend to form tightly packed, rigid monolayers with high phase transition temperatures, often mimicking the ordered domains found in eukaryotic membranes or the *gel* phase. In contrast, unsaturated lipids (e.g., DOPC, POPG), which contain *cis*-double bonds that create *kinks* in the hydrocarbon chains, prevent tight packing and maintain the membrane in a liquid-disordered (fluid) state at physiological temperatures. This fluidity is a hallmark of most bacterial inner membranes and facilitates the penetration of amphiphilic peptides by reducing the energy cost of insertion. Therefore, incorporating unsaturated lipids into monolayer models is essential to accurately reproduce the viscoelastic properties and the susceptibility to disruption characteristic of native biological membranes.

The phase behavior of lipid membranes is a key determinant of how antimicrobial peptides interact with and disrupt lipid interfaces. Depending on lipid composition and environmental parameters such as temperature, bilayers can transition between distinct phases, including the tightly packed gel phase (Lβ), which exhibits low lateral mobility and strong resistance to peptide insertion, and the more disordered fluid phase (Lα), which favors molecular diffusion and facilitates AMP penetration [75]. In mammalian cells, cholesterol promotes the formation of the liquid-ordered phase (Lo), which maintains a balance between fluidity and rigidity, making membranes more resistant to AMP-induced disruption [76]. Conversely, bacterial and diseased mammalian membranes, which often have lower cholesterol content, are characterized by higher fluidity and increased susceptibility to AMP interactions [77].

A variety of biomimetic membrane models have been developed to investigate AMP–membrane interactions, each offering distinct advantages depending on the level of complexity and resolution required [24–26] (Fig. 3A). Liposomes, self-assembled lipid vesicles that encapsulate an aqueous core, are widely used due to their resemblance to natural cell membranes. SUVs provide a homogeneous system for kinetic studies, while LUVs better replicate the lipid packing found in cell membranes. GUVs, due to their larger size, enable real-time visualization of AMP-induced membrane disruption through microscopy techniques. In general, lipid vesicles are commonly used to mimic bilayer curvature, composition, and encapsulation properties. SLBs and black lipid membranes (BLMs) enable complementary approaches for probing AMP-induced binding, insertion, or pore formation. While these models provide valuable functional and mechanistic information, they can be limited by factors such as substrate effects or structural fragility. In contrast, lipid monolayers formed at the air–water interface offer a uniquely accessible and tunable framework for dissecting the fundamental physicochemical determinants of AMP–lipid interactions [33] (Fig. 3B). The Langmuir trough technique enables precise control over lipid composition, lateral packing, and surface pressure, allowing researchers to systematically investigate how these parameters influence peptide adsorption, insertion, and membrane perturbation. By compressing monolayers to biologically relevant surface pressures, it is possible to mimic the lateral densities characteristic of cellular membranes and establish direct correlations between AMP ISA and interfacial organization.

Lipid monolayers offer several advantages over bilayer models. Their experimental setup enables direct measurement of interfacial parameters such as surface pressure and molecular area [78,79], while thermodynamic quantities like the Gibbs free energy of adsorption can be inferred from these measurements, providing quantitative insights into AMP binding affinity and membrane-disruptive potential. In addition, real-time visualization techniques such as Brewster angle microscopy (BAM) and IRRAS enable researchers to monitor structural changes and peptide-induced disruptions with high spatial and temporal resolution. Monolayers also facilitate the study of the effects of environmental parameters such as pH, ionic strength, and temperature on peptide-lipid interactions, offering valuable data for the design of AMPs with enhanced specificity and antimicrobial activity.

Despite their advantages, lipid monolayers have limitations. They lack the bilayer asymmetry and lateral heterogeneity found in natural membranes, which are crucial for fully replicating biological environments. Additionally, monolayers do not allow the study of transmembrane processes such as peptide translocation or bilayer flipping. However, when used in conjunction with other biomimetic models, monolayers provide critical mechanistic insights that complement findings from more complex systems.

Altogether, monolayers can be seen as reductionist outer membrane models that emphasize lateral packing, charge density and leaflet-specific effects. When interpreted together with GUV leakage assays, SLB electrical measurements or vesicle-based calorimetry, they help disentangle which steps of the AMP mechanism are primarily controlled by interfacial thermodynamics and which ones require full bilayer integrity or transmembrane topology. Throughout this review we highlight specific cases where monolayers have revealed trends that were not apparent from vesicle experiments alone, as well as situations where monolayer data must be interpreted with caution.

4. Self-assembly and organization of antimicrobial peptides at interfaces

AMPs have a remarkable ability to self-assemble at interfaces, leveraging their amphiphilic, cationic properties to drive adsorption and functional organization. This self-assembly process is highly dependent on the nature of the interface—whether air-water, lipid monolayers, or supported systems—and has been extensively investigated using techniques such as Langmuir trough, X-ray reflectivity (XR), grazing-incidence X-ray diffraction (GIXD), and various spectroscopic and microscopic approaches [80,81].

Amphiphilicity and charge distribution are critical factors influencing AMP adsorption, allowing peptides to orient their hydrophobic and charged residues in a configuration optimized for interacting with lipid interfaces or aqueous environments. Experimental studies have revealed that AMP interfacial behavior is influenced by a complex interplay of lipid type present at the interface, peptide structure, packing density, and environmental conditions, all of which modulate their antimicrobial activity and selectivity [40].

4.1. Mechanisms of peptide adsorption at interfaces

AMP adsorption mechanisms depend largely on the specific interface to which they are exposed. At air-water interfaces in the absence of lipids, AMPs spontaneously form monolayers by adopting an amphiphilic orientation, with hydrophobic residues facing the air phase and hydrophilic residues interacting with the aqueous subphase. This behavior is supported by Langmuir trough studies, which show an increase in surface pressure upon AMP adsorption, leading to expanded molecular areas and structural rearrangements [29,30,38,39,82]. For instance, PG-1 forms stable monolayers at the air-water interface while undergoing structural transitions, such as folding into β-sheet conformations, which has been confirmed through GIXD and XR experiments [39,41]. Likewise, Trichogin GA IV (TRIC) was also proved by molecular dynamics simulations to form α-helices, β-sheets and random coils at different states of compression [83]. These structural transitions enhance the AMP membrane-disruptive capabilities by facilitating deeper insertion upon contact with lipid interfaces. Similarly, Ar-1 form ordered monolayers, aligning their β-sheet structures parallel to the

interface, optimizing their amphiphilic interactions and stabilizing the monolayer [38].

On lipid monolayers, AMP adsorption mechanisms are primarily governed by a combination of electrostatic interactions (between positively charged AMPs and negatively charged lipid headgroups like DPPG) and hydrophobic insertion into the lipid tail region. Multiple studies confirm that charge balance between the peptide and lipid headgroups is critical for binding. For instance, LL-37 and SMAP-29 exhibit strong interactions with the anionic lipid DPPG but much weaker affinity for zwitterionic lipids such as DPPC [36,41,84]. Similar findings were obtained by Langmuir trough and IRRAS experiments for the KLA1 antimicrobial peptide, which adsorbed pronouncedly to anionic monolayers but not to zwitterionic lipids [47]. This selective affinity highlights the crucial role of lipid composition in AMP specificity and provides insight into their mechanism of selective antimicrobial activity.

In both air-water and lipid monolayer systems, peptide concentration and surface pressure critically influence adsorption dynamics. At low peptide concentrations, AMPs tend to spread evenly across the interface, while at higher concentrations, aggregation and multilayer formation can occur, which may hinder their biological efficacy [46].

4.2. *Influence of environmental parameters on AMP self-assembly and organization*

The structural organization and functional performance of AMPs at interfaces are highly sensitive to environmental parameters, including pH, ionic strength, and temperature, which influence peptide conformation, adsorption kinetics, and interfacial stability (Fig. 4).

The protonation state of AMP residues is pH-dependent and significantly affects their adsorption and orientation [85]. Acidic pH conditions enhance electrostatic attraction between cationic peptides and anionic lipid headgroups, promoting tighter binding and improved structural stability. This effect has been demonstrated for LL-37 and its fragments, which display increased surface adsorption and conformational stability under acidic conditions compared to neutral pH [45,86]. This phenomenon is especially important when the membrane phospholipid composition includes acidic headgroups such as those of DPPG or cardiolipin, since they interact more favorably with cationic peptides at lower pH.

Electrostatic interactions between AMPs and lipid monolayers are also strongly influenced by the ionic strength of the surrounding medium. Low ionic strength conditions reduce electrostatic screening, leading to stronger peptide-lipid interactions and deeper penetration into the lipid monolayer, as confirmed by fluorescence microscopy and surface pressure-area isotherms [46,87]. Conversely, high ionic strength can weaken peptide-lipid binding by shielding electrostatic attractions, although in some cases, it may promote peptide clustering and cooperative interactions at the interface [32,88].

Temperature variations affect lipid packing, AMP structure and mobility, and phase behavior. Higher temperatures typically induce membrane disorder, facilitating deeper AMP insertion and enhancing their membrane-disruptive potential. For instance, studies on SMAP-29 have shown a strong correlation between increased temperature and peptide-induced fluidization of lipid monolayers, with compression modulus analysis and BAM imaging confirming AMP-induced phase transitions [84]. However, excessive temperatures may also destabilize AMP secondary structures, leading to reduced efficacy [46,89,90].

4.3. *Importance of lateral packing density and spatial orientation*

The functionality of AMPs in monolayers is critically influenced by their lateral packing density and spatial orientation at the interface, which are tightly related to monolayer phase behavior. This lateral organization translates directly into mechanical properties such as membrane stiffness and elasticity. Although the quantitative thermodynamic definition of these parameters is detailed later in Section 5.2, it is crucial to understand conceptually that high interfacial rigidity acts as a physical barrier to peptide insertion, whereas fluid, elastic states facilitate the cooperative defects necessary for AMP activity. These factors determine the cooperative behavior of AMPs, modulating key mechanisms such as synergistic pore formation, membrane disruption, and steric hindrance. At high monolayer packing, the surface pressure is very sensitive to area changes, molecules present low lateral mobility and strong resistance to peptide insertion, consequently reducing antimicrobial efficacy. However, at very fluid and disordered states, the molecules diffusion is enhanced, which facilitates AMP insertion and the monolayer disruption. Experimental data derived from π-A isotherms of AMP-lipid monolayers, in particular of LL-37 and protegrin-1, have revealed optimal packing and fluidization conditions that maximize ISA while avoiding steric limitations [36,46,84]. In these studies, moderate surface pressures and fluidize states of the monolayer facilitate the formation of AMP-rich domains that allow cooperative insertion into lipid monolayers, whereas excessive compression leads to steric exclusion effects that impede deep membrane penetration and antimicrobial action.

Spatial orientation at the lipid interface is equally crucial in dictating AMP functionality. Peptides that align parallel to the membrane surface maximize their interactions with lipid acyl chains, optimizing their capacity to destabilize membrane integrity. This behavior has been observed in β-sheet-forming AMPs, such as protegrin-1, where XR studies have demonstrated a strong preference for parallel alignment with lipid headgroups in DPPG monolayer [39,41]. Such alignment enhances the amphiphilic interaction of the peptides, promoting deeper penetration and increased disruption of the lipid structure.

Amphiphilic α-helical peptides, such as arenicins, exhibit a

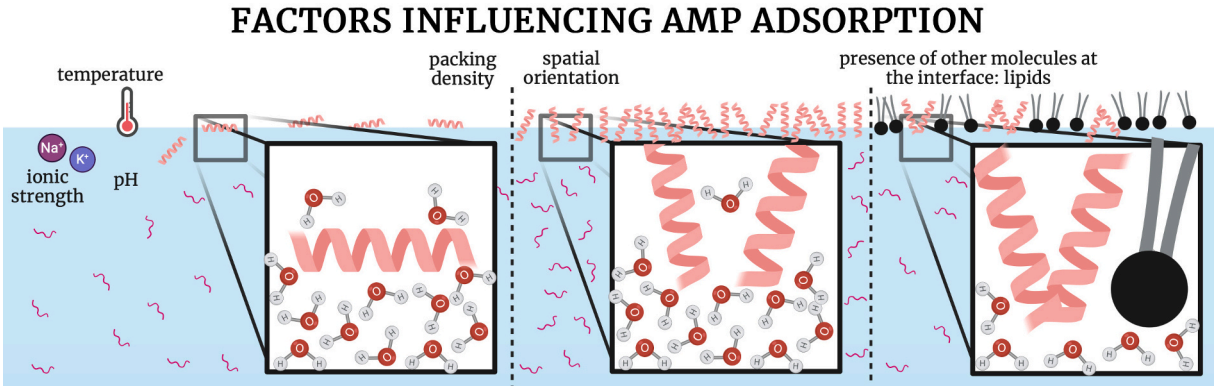

Fig. 4. Scheme of the different factors influencing AMP adsorption to air-water interfaces and lipid monolayers: packing density and spatial orientation of the molecules at the interface and environmental parameters such as pH, ionic strength and temperature.

remarkable degree of structural plasticity, transitioning between α-helical and intermolecular β-sheet conformations in response to changes in surface pressure and lipid composition. Compression studies have shown that arenicins initially adopt a helical conformation parallel to the interface, but upon increasing surface pressure, they transition to β-sheet arrangements that enhance surface coverage and membrane perturbation [38,39]. These structural adaptations suggest that AMPs can dynamically reorganize to optimize their interactions with lipid interfaces under varying physiological conditions.

5. Thermodynamic insights into lipid monolayers in the presence of antimicrobial peptides

The thermodynamic characterization of lipid monolayers in the presence of AMPs provides essential insight into their interfacial organization, packing behavior, and phase transitions. These molecular-scale properties are critical for understanding how AMPs interact with lipid assemblies, influencing both their selectivity and capacity for membrane disruption. Together, they offer a quantitative framework for characterizing AMP-induced perturbations at interfaces and support the rational design of peptides with tailored membrane-interactive properties. The following sections examine in detail the thermodynamic parameters, interfacial equations of state, and mixing behaviors that define AMP-lipid systems.

5.1. Fundamental thermodynamic parameters governing AMP-lipid interactions

At a liquid–gas interface, surface tension is defined as the reversible work required to increase the interfacial area at equilibrium per unit area and reflects the balance of cohesive forces between molecules in surface. The adsorption of other molecules to the interface provokes the reorganization of molecules and a change in the strength of cohesive interactions in the surface region, which modifies surface tension. The amount and direction in which surface tension is altered depends on the nature of interactions between the adsorbed and the surface molecules.

For AMPs at the air-water interface, AMP adsorption typically reduces surface tension due to their amphiphilic nature, with hydrophilic domains interacting with water and hydrophobic regions oriented toward air, lipid tails, or adjacent amphiphiles. The thermodynamics of AMP adsorption to the air-water interface can be captured by the general Gibbs adsorption isotherm, which is derived from the general expression for the Gibbs free energy (G) of the surface region and the fundamental thermodynamic relation for the internal energy (dU):

$$\Gamma = -1/\mathrm{RT}\ \partial\gamma/\partial \ln \mathrm{C} \quad (1)$$

where Γ is the surface excess concentration of AMP molecules, C the bulk phase concentration of AMP molecules, R is the universal gas constant and T is the absolute temperature [91]. The Gibbs adsorption isotherm relates changes in surface tension upon AMP adsorption or desorption with their concentration at the bulk phase. From AMP adsorption, the average molecular area of AMPs in surface ($A_{peptide}$) can also be obtained with the expression $A_{peptide} = \frac{1}{\Gamma N_A}$, where N_A is the Avogadro number. Eq. 1 is valid for concentration ranges below the critical micellar concentration (CMC), where AMPs can be either at bulk phase or adsorbed at surface but not forming micelles. Above the CMC, it is not possible to predict if AMPs will go to micelles, to the interface, or stay at the bulk region. Strictly speaking, Eq. 1 assumes ideal behavior where the activity coefficient is unity. In crowded interfaces where adsorbed molecules interact strongly, activity corrections are required [92]. Moreover, in mixed lipid–peptide systems, the interplay between electrostatic and hydrophobic forces drives complex reorganization events that go beyond simple adsorption. Crucially, high local concentrations of AMPs can induce the extraction of lipids into the subphase (detergent-like effect) or the formation of pores. These phenomena irreversibly alter the surface composition, violating the equilibrium assumptions of Eq. 1 and causing the relationship between surface tension and bulk concentration to deviate significantly from the theoretical prediction.

In the presence of lipidic monolayers the magnitude and direction of the change in surface tension due to AMP adsorption depends on the lipid composition, the organization of the interface, the extent of AMP adsorption and the AMP-lipid interplay [47]. This change reflects the AMP adsorption and the balance between AMP-induced stabilization or disruption of lipid packing. As a general trend, when AMPs provoke the reorganization of the lipid layer the system stabilizes, minimizing interfacial free energy, and the surface tension is reduced. On the contrary, when AMPs disrupt and destabilize the lipid organization of the interface, the surface tension increases or remains at the same value. The amphiphilic properties and charge characteristics, such as the strong cationic nature of certain AMPs, significantly influence the adsorption density, and, consequently, their effect on interface properties, which is related to their antimicrobial efficacy at interfaces [35,40].

Surface pressure (π) is the difference between the surface tension of a clean air-water interface (γ_0) and that of the interface when it is covered by a molecular film (γ), such as a lipid monolayer, AMPs or their mixtures ($\pi = \gamma_0 - \gamma$). It quantifies the reduction in free energy per unit area, or surface tension, due to the presence of adsorbed molecules. For lipid-AMPs mixtures, analogously to surface tension, surface pressure provides insights into cooperative or competitive behaviors, such as lipid-peptide interactions, monolayer stability, and potential BAA. Surface pressure-area isotherms (π–A) are a cornerstone of Langmuir trough studies and provide key information about molecular packing, monolayer stability, and phase behavior. π–A isotherms describe how the surface pressure varies with the average area per molecule or surface concentration, either AMP or lipid, at the interface. This leads to a fundamental distinction in how surface tension is modulated in experimental setups. In Gibbs adsorption, γ changes spontaneously due to the equilibration of soluble molecules between the bulk and the interface (concentration-driven). In contrast, in Langmuir compression isotherms, γ changes because the available surface area is mechanically reduced for a fixed number of effectively insoluble molecules (area-driven). Consequently, the classical Gibbs equation (Eq. 1) does not directly apply to standard compression isotherms, which assume a closed system at the interface. However, for AMPs—which are often water-soluble and dynamic—this boundary becomes less clear: high surface pressures can force peptide desorption or squeeze-out into the subphase, reintroducing bulk exchange and complicating the thermodynamic analysis.

Several regions of the π-A isotherm correspond to distinct organizational and structural states of the monolayer, which typically consists of AMPs alone or mixtures of AMPs and lipids. These regions are observed during the compression process [93–95] (Fig. 5):

- Gas-like (G): At low surface pressures and large molecular areas, the monolayer components (AMPs, lipids, or both) are sparsely

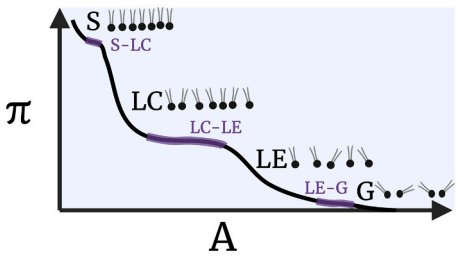

Fig. 5. Diagram of the π-A isotherm of a lipid monolayer under compression indicating the different monolayer phases: S, LC, LE and G. Phase transition regions are highlighted in a purple shadow, corresponding to π *plateau* regions. (For interpretation of the references to colour in this figure legend, the reader is referred to the web version of this article.)

distributed and weakly associated. In this region, AMPs may be unfolded or disorganized at the interface, while lipids remain in a disordered state.

- Liquid-expanded (LE): As the monolayer is compressed, AMPs begin to interact with each other and with lipids. Electrostatic and hydrophobic forces drive the organization of AMPs into secondary structures (e.g., α-helices) and promote lipid-AMP interactions. The LE region reflects partial lateral cohesion, with AMPs and lipids forming a loosely organized arrangement.
- Liquid-condensed (LC): Further compression forces the monolayer components into a tightly packed arrangement. In this region, AMPs and lipids exhibit stronger lateral interactions. For AMP-lipid mixtures, this may include lipid-induced alignment of AMPs or AMP-mediated ordering of lipid molecules. Specific structural motifs, such as β-sheets in AMPs or lipid domain formation, may emerge.
- Solid (S): At high surface pressures, the monolayer presents an even more tightly packed state.
- Collapse: At very high surface pressures, the solid state might lead to the monolayer instability. Components may be expelled from the interface, or multilayered structures may form due to the breakdown of the monolayer integrity. In mixed systems, this could involve the segregation of AMPs and lipids or the formation of complex multilayered aggregates.

The transitions from LE to LC states often correspond to critical structural rearrangements in AMPs, such as folding into secondary structures, reorientation (e.g., tilting), or the establishment of hydrogen-bonded networks. These structural transitions are pivotal in modulating AMP-lipid interactions within biological membranes and can significantly influence their antimicrobial activity and efficacy [35,46,84]. According to the Gibbs phase rule, monolayer phase transitions are manifested in the isotherms by a constant surface pressure region, which might sometimes differ from a constant value due to phase domain formation.

To identify phase coexistence or pure phase regions is sometimes convenient to analyze the change in surface pressure due to area compression, reflected in the definition of the compressibility modulus of the monolayer (C_s), which describes the monolayer stiffness [96,97]:

$$C_s^{-1} = -A\frac{\partial \pi}{\partial A} \tag{2}$$

The compressibility or elasticity modulus indicates the resistance that the monolayer exerts to compression while providing information about phase behavior. A minimum in the compressibility isotherms indicates a phase transition, while an increase in lipid rigidity would be expressed as a maximum in C_s^{-1}. In the ideal case of mixing, the compressibility modulus would be a linear combination of the compressibility modulus in the only-lipids and only-peptides case. The presence of the peptides at the interface could suppose a change in the monolayer compressibility and phase transitioning at certain surface pressure values.

Soft monolayers (low C_s^{-1}) dominate in the LE region, whereas stiff monolayers (high C_s^{-1}) emerge in ordered or LC phases, presenting higher resistance to compression. This property reveals the adaptability of lipid monolayers containing AMPs under mechanical forces, e.g. during bacterial membrane disruptions. Authors often employ compressibility modulus thresholds to assign monolayer phases. Usually, the compressibility range 0–12.5 mN/m is identified with G phase, 12.5–100 mN/m to LE, 100–250 mN/m to LC and $>$ 250 mN/m to S [98,99].

When AMPs interact with lipid monolayers or bilayers, including biological membranes, three different behaviors can be observed in π-APL isotherms after peptide injection [92]: 1) a pure lipid monolayer-like behavior, when no changes are seen with respect to the only-lipids monolayer; 2) a protein aggregate-like behavior, when the isotherm of the lipidic monolayer in the presence of peptide has the same behavior as in the absence of lipids (air-water interface); and 3) a mixed protein-lipid monolayer-like behavior, when the shape of the isotherms differs from both pure monolayer of lipid and peptide. Indeed, in some lipid-AMP mixed monolayer two surface pressure *plateaus* might be seen at low APL values, which would probably correspond to the collapse pressures of the peptide-enriched phase and the lipid-enriched phase, characteristic of the ideal mixing behavior [100]. The behavior of mixed AMP-lipids systems can often be described using thermodynamic quantities such as the Gibbs free energies of mixing and mixing enthalpies:

$$\Delta G_{mix} = \Delta H_{mix} - T\Delta S_{mix} \tag{3}$$

Negative ΔG_{mix} values indicate favorable AMP-lipid interactions, typically driven by electrostatic attraction between cationic peptides and anionic lipids (e.g. DPPG); while positive ΔG_{mix} describe phase separation or incompatibility, often seen in AMP interactions with zwitterionic lipids (e.g. DPPC). The Gibbs free energy of mixing can be obtained from π-A isotherms in terms of the excess (ΔG_{exc}) and ideal (ΔG_{ideal}) Gibbs energy, with the following expressions:

$$\Delta G_{mix} = \Delta G_{exc} + \Delta G_{ideal} \tag{4.a}$$

$$\Delta G_{exc} = \int_0^{\pi} A_{exp} - (A_1 x_1 + A_2 x_2) d\pi \tag{4.b}$$

$$\Delta G_{ideal} = RT(x_1 \ln x_1 + x_2 \ln x_2) \tag{4.c}$$

where A_{exp} is the molecular area values in the isotherm with the mixed system, A_i the molecular area values in the isotherm of a monolayer containing only the i component and x_i the molar fraction of each component in the mixture [101].

In general, the partitioning of solute molecules between two different phases or interface regions, for example, the partitioning of AMPs between the water bulk and the air-water interface (where might be located a lipidic monolayer) is driven by Gibbs free energy changes associated to AMP adsorption. The relation between changes in Gibbs free energy and the partitioning of AMPs is derived from the partition function of the system as [102]:

$$\Delta G_{ads} = -RT\ln K \tag{5}$$

where K represents the dimensionless partition coefficient. Since adsorption involves a transition from a 3D bulk to a quasi-2D interface, defining K rigorously requires treating the interface as a phase with a defined volume. This is typically achieved by using the lipid molar volume (v_L) [102] or, equivalently, assuming an effective interfacial thickness (δ). Under this convention, the concentration at the interface is defined as Γ/δ (or related to the mole fraction via v_L), allowing K to be expressed dimensionless as $K \approx \Gamma/(C_{bulk}\delta)$. While AMP adsorption to the interface (and the subsequent formation of an AMP monolayer or insertion to a lipid monolayer) is driven by favorable enthalpic interactions (electrostatic and hydrophobic), desorption is entropically favored due to the increased conformational and translational freedom of peptides in solution. A negative Gibbs free energy of adsorption (ΔG_{ads}) indicates that AMP adsorption occurs spontaneously.

At the molecular level, the favorable ΔG_{ads} and ΔG_{mix} associated with AMP-lipid interactions are driven by a complex balance of enthalpic and entropic contributions. Beyond the primary electrostatic attraction between cationic residues and anionic headgroups, the entropic gain resulting from the release of structured water molecules from the peptide and lipid solvation shells (the hydrophobic effect) serves as a major thermodynamic driver for peptide insertion. Furthermore, the formation of specific hydrogen-bonding networks between the peptide backbone and the lipid phosphate or carbonyl groups provides additional enthalpic stabilization, which dictates the final orientation and structural stability of the peptide at the interface.

Of course, this is an oversimplified description of the general interaction mechanism between peptides and lipid monolayers or bilayers but the structure, assembly pattern and the value of all these thermodynamic properties depends critically on the peptide sequence and lipid composition.

5.2. Equations of state for lipid monolayers in the presence of antimicrobial peptides

Two-dimensional equations of state (2D EoS) or surface equations of state (SEoS) provide a mathematical framework to describe the relationship between surface pressure, molecular area, and thermodynamic properties of molecular monolayers at interfaces such as the air/water interface. By utilizing experimental techniques such as Langmuir trough studies to produce π–A isotherms, SEoS can be applied to investigate the physicochemical behavior of AMPs in monolayers, both in lipid-free conditions and when interacting with lipid-containing monolayers. These studies can potentially reveal peptide organization, interfacial packing, and interactions with lipids, which are critical for understanding the conditions under which AMPs' biological mechanisms of action happen. These models have been sparsely applied to AMPs, so their use for characterizing AMP-lipid monolayers remains relatively limited. Simple models, like the ideal gas 2D EoS [103], assume non-interacting molecules, providing only basic insights. Extensions such as the Volmer equation [104] and van der Waals-type model [104–107] incorporate molecular packing, finite molecular area, and intermolecular interactions, enabling the study of peptide organization and lipid interactions. Advanced approaches, including virial expansions and Helfrich elasticity theory [108,109], account for non-ideal behavior and curvature effects, offering perspectives on phase transitions and monolayer bending. Lennard-Jones potential-based models and mean-field approaches address specific interactions, such as amphiphilic aggregation and electrostatic contributions. Many other SEoS have been developed and tested for monolayers of biomolecules [103,110–115]. Despite their theoretical relevance, many of these models remain underutilized in experimental studies of AMP-lipid monolayers, with their full potential yet to be realized in elucidating peptide mechanisms at interfaces.

6. Methods to characterize lipid monolayers in the presence of AMPs

The characterization of AMP-perturbed lipid monolayers requires experimental and computational techniques capable of resolving changes in interfacial thermodynamics, mechanical response, molecular structure, and mesoscale organization. Together, these measurements provide the quantitative basis to link macroscopic observables (such as shifts in π–A isotherms, viscoelastic signatures, or domain morphologies) with the molecular mechanisms of AMP adsorption, insertion, aggregation, and lipid reorganization discussed in previous sections.

In this section, we organize the most widely used approaches to interrogate AMP–lipid monolayers into five complementary families: (i) Langmuir trough–based methods, which quantify interfacial thermodynamics, mechanical response, and surface potentials; (ii) interfacial rheology, which resolves frequency-dependent viscoelastic behavior; (iii) spectroscopic techniques, providing molecular-level information on structure, orientation, and hydration; (iv) microscopy methods, which visualize lateral heterogeneity and peptide-induced domain remodeling; and (v) computational approaches, mainly MD and multiscale models, which offer atomistic to mesoscale insight and a bridge to theory. Fig. 6

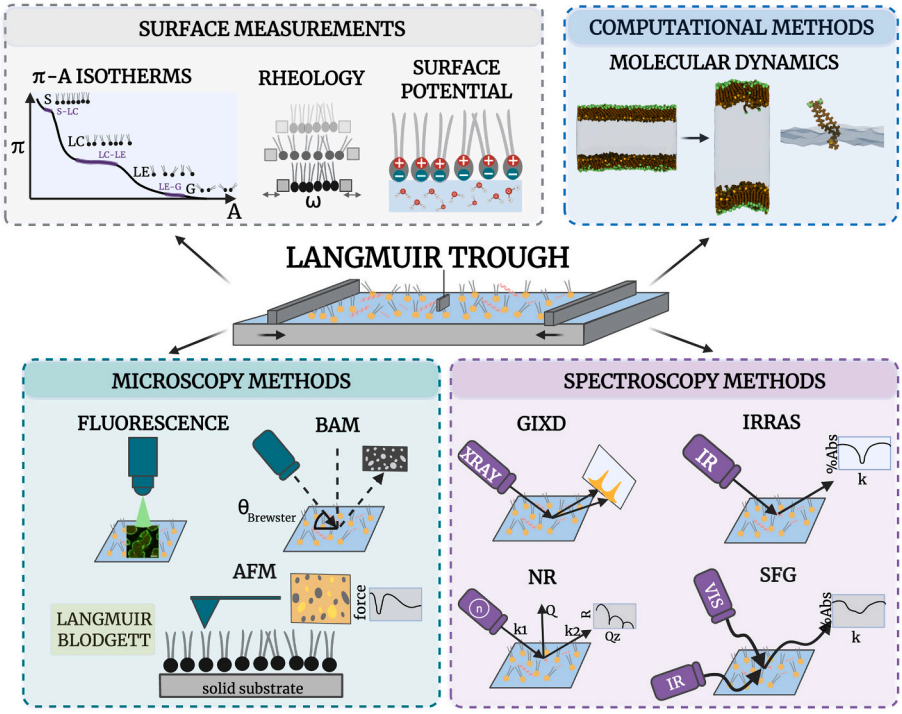

Fig. 6. Comprehensive schematic of experimental and computational approaches for characterizing Langmuir monolayers. The central Langmuir trough acts as the fundamental platform for forming and manipulating amphiphilic monolayers at the air-water interface, serving as the hub for four primary analytical pillars. The top-left panel, Thermodynamics and Rheology, groups measurements of macroscopic physical properties, including surface pressure-area (π-A) isotherms, surface potential, and interfacial shear rheology. The top-right panel, Computational Methods, illustrates the use of theoretical simulations, such as molecular dynamics, to model behavior at the nanoscale. The bottom panels detail techniques for structural and morphological analysis: Microscopy Methods (bottom-left) enable visualization of domains in situ (Fluorescence, BAM) and allow for topographic analysis following Langmuir-Blodgett transfer onto solid substrates (AFM); Spectroscopy Methods (bottom-right) are employed in situ to determine crystalline packing (GIXD), vertical profiles (NR), and molecular orientation and composition at the interface (IRRAS, SFG).

summarizes the experimental and computational tools most commonly coupled to Langmuir trough platforms. Table 2 compiles the experimental techniques, detailing what each method measures, the observables it yields, and the mechanistic information that can be extracted. Table 3 provides a parallel framework that links these experimental observables with their computational counterparts, highlighting the MD-derived descriptors that quantify the same interfacial mechanisms.

6.1. Langmuir trough techniques

Langmuir trough methodologies constitute the core experimental framework for characterizing AMP–lipid monolayers [115]. They provide direct access to the primary interfacial observables, molecular area (A) and surface tension, from which thermodynamic, mechanical, and dipolar properties are quantified. These measurements form the basis of the analyses developed in Sections 6.1.1–6.1.4.

In a typical experiment, a lipid monolayer is spread at the air–water interface and compressed at a controlled rate while π is monitored with a Wilhelmy plate [116–118], producing characteristic π–A isotherms. AMPs can be incorporated either by co-spreading peptide–lipid mixtures or, alternatively, by injecting the peptide into the subphase beneath a preformed lipid film [119–121]. The choice of protocol allows one to isolate different aspects of peptide–lipid interactions, including insertion into packed monolayers, adsorption from bulk solution, and peptide-induced restructuring of lipid phases. Combined with controlled cycling, fixed-area adsorption measurements, and surface potential detection, Langmuir trough experiments enable a comprehensive evaluation of AMP effects on monolayer packing, stability, and interfacial organization.

6.1.1. Thermodynamic signatures in π–A isotherms

Recording π–A isotherms under controlled compression–expansion cycles provides the primary thermodynamic readout of AMP–lipid interactions. Characteristic signatures include shifts in lift-off area, changes in mean molecular area, modifications of the slope of the liquid-expanded (LE) and liquid-condensed (LC) regions, the appearance or displacement of LE–LC plateaus, kinks associated with phase transitions, and altered collapse pressures. These features are originated from changes in molecular packing and reveal how AMPs modulate the free-energy landscape of the monolayer.

Peptide binding typically perturbs the balance between entropic chain disordering and enthalpic lipid–lipid interactions, giving rise to expanded isotherms, reduced plateau slopes, or destabilization of condensed phases. Conversely, AMPs that stabilize hydrocarbon packing or that insert cooperatively may shift the isotherm toward smaller areas or increase collapse pressure. A representative example of this stabilizing effect is seen in the human cathelicidin fragment LL-32, which forms robust α-helical monolayers capable of sustaining surface pressures up to 24 mN/m, whereas shorter fragments like LL-20 fail to maintain interfacial stability under the same conditions [176]. The degree of non-ideal mixing in mixed AMP–lipid systems is especially pronounced in monolayers containing anionic bacterial lipids such as DPPG, in contrast with zwitterionic DPPC, reflecting lipid-dependent selectivity of peptide interactions [119,121]. At higher surface pressures, peptides can undergo compression-induced reorganization at the interface, including clustering or partial ordering into α-helical or β-sheet conformations. These processes are strongly peptide- and packing-dependent. Such structural rearrangements, however, cannot be inferred unambiguously from the isotherm alone; they require complementary spectroscopic confirmation using IRRAS or circular dichroism (CD), which can resolve secondary structure formation and peptide orientation at the interface [119,121].

Taken together, the thermodynamic fingerprints extracted from π–A isotherms provide a quantitative framework for identifying AMP-induced modifications of phase behavior, mixing thermodynamics, and insertion propensity, which are further refined by mechanical, spectroscopic, and microscopic measurements described below.

6.1.2. Mechanical response: compressibility modulus and hysteresis

The compressibility modulus, obtained from numerical differentiation of the π–A isotherm (Eq. 2), quantifies the elastic response of the monolayer to compression [96,97]. High C_s^{-1} values correspond to rigid, tightly packed films with reduced hydrocarbon-chain mobility, whereas low C_s^{-1} indicates fluidized or disordered states. These physical states are defined by specific numeric ranges: values between 12.5 and 100 mN/m characterize the LE phase, whereas the LC phase exhibits values between 100 and 250 mN/m, and the S state is identified by values exceeding 250 mN/m [98,99]. AMP binding typically lowers C_s^{-1} by disrupting chain packing, destabilizing condensed phases, or generating peptide-enriched fluid domains; however, peptides that stabilize packing or insert cooperatively may increase C_s^{-1} or shift the onset of condensed phases.

Beyond this quasi-equilibrium elastic response, dynamic compression–expansion cycles reveal the kinetic and dissipative aspects of AMP-induced perturbations. Enlarged hysteresis loops reflect energy dissipation associated with peptide clustering, rearrangement of lipid phases, irreversible peptide insertion, partial squeeze-out from condensed regions, or lipid extraction during cycling. Narrow loops, in contrast, indicate predominantly elastic and reversible behavior. Thus, hysteresis provides a complementary perspective on the stability and reversibility of AMP–lipid interactions that cannot be inferred from C_s^{-1} alone.

Collapse pressure adds a third mechanical descriptor. In AMP-containing monolayers, increased collapse pressure can indicate stabilizing AMP–lipid interactions, whereas reductions may signal chain disordering or destabilization of condensed phases. Because collapse is sensitive to steric packing geometry and compression rate, its interpretation must be cross-validated with C_s^{-1} and hysteresis signatures.

Together, compressibility analysis, hysteresis behavior, and collapse pressure form a coherent mechanical fingerprint of AMP action, distinguishing whether peptides act primarily as disordering agents, stabilizers, or dynamic remodelers of interfacial structure.

6.1.3. Peptide adsorption from the subphase: Gibbs adsorption isotherms

In addition to probing the mechanical consequences of peptide binding, Langmuir troughs can quantify the thermodynamic driving forces of AMP adsorption. This is achieved by measuring the change in surface tension as a function of bulk peptide concentration while keeping the monolayer in a well-defined interfacial state, typically at fixed molecular area or fixed surface pressure. Under these conditions, peptide molecules adsorb to the interface and induce a concentration-dependent decrease in γ. From the variation of γ with concentration, the surface excess Γ can be obtained using the Gibbs adsorption equation (Eq. 1), yielding the adsorption isotherm $\Gamma(C)$. Fitting $\Gamma(C)$ to a Langmuir-type model [122]:

$$\Gamma(C) = \Gamma_{max}\frac{KC}{1+KC}, \tag{6}$$

provides the maximum interfacial peptide coverage (Γ_{max}) and an adsorption or partitioning constant K. Under dilute conditions where peptide activity approximates its bulk concentration, K quantifies peptide affinity for the interface, and the corresponding standard free energy of adsorption can be derived (Eq. 5). Deviations from the Langmuir form at higher surface coverage or in the presence of lipid–peptide interactions may require more complex models such as Frumkin or Szyszkowski isotherms.

Performing these experiments at different initial surface pressures (i.e., different packing states of the lipid monolayer) enables direct evaluation of how lipid organization modulates AMP accessibility. Peptides generally adsorb more readily onto expanded or disordered monolayers, whereas densely packed films restrict adsorption and may reveal cooperative effects or competition between peptide insertion and surface crowding. Thus, Gibbs adsorption measurements complement π–A

Table 2
Experimental techniques to characterize lipid monolayers and their interactions with AMPs.

Technique		Measurement	Information provided	Obtained by	Comments
Surface	Langmuir trough	π-A isotherms	Response to compression: compressibility modulus, C_S^{-1}	Numerical derivation of the isotherm $C_S^{-1} = -\,\mathrm{A}\,\partial\pi/\partial\mathrm{A}$	Assumes quasi-equilibrium; sensitive to compression rate
			AMPs surface excess concentration, Γ	Gibbs adsorption equation, $\Gamma = -1/\mathrm{RT}\partial\gamma/\partial\ln\mathrm{C}$	Valid for dilute, ideal adsorbates; corrections required for non-ideal interactions
			Molecular area per AMPs, A	$A = 1/\Gamma N_A$ (for Gibbs monolayers). A is the independent variable for Langmuir monolayers	Accuracy depends on Γ determination
			AMPs partitioning constant, K	Langmuir/Szyszkowski isotherm, $\Gamma = \Gamma_{max}KC/(1+KC)$	Assumes low surface coverage; may require Frumkin correction
			Kinetics of AMPs adsorption to the surface	π-t relaxation curves; exponential or stretched-exponential fits	Distinguishes diffusion-limited vs. reorganization-limited adsorption
		Compression-expansion cycles	Hysteresis energy and reversibility	Energy dissipation; packing transitions	Area difference between compression/ expansion branches
	Surface potential	ΔV-A isotherms	Apparent dipole moment	Maximum value of surface potential, $\mu_\perp^A = \varepsilon_0 A \Delta V_{max}$	Requires stable monolayers. The interpretation depends on dipole-layer model
			Molecular reorientation after AMP adsorption	Changes in ΔV and $\mu_\perp^A$	
Microscopy	BAM	Reflected polarized light under Brewster angle	Monolayer morphology and phase coexistence domains	Contrast due to refractive index differences	Non-invasive; optimal for Langmuir-trough
	AFM	Monolayer topography	Morphology and phase domains; height contrast; peptide-induced restructuring	Z-profile from tapping/AC mode	Requires a solid substrate: by Langmuir-Blodgett or SAM grown from solution (possible tip-induced deformation). Resolution limited by substrate roughness
			Thickness at different locations	Steep-height analysis	
	Fluorescence	Fluorescence emission patterns	Morphology, phase domains	Fluorophore intensity contrast	On Langmuir-trough or on SAM on solid substrates; possible photobleaching.
			Peptide partitioning constant, K	Ratio of fluorescence in coexistence phases; kinetic fits $\tau = \frac{\tau_W + Kx_L\lvert L\rvert\tau_L}{1+Kx_L\lvert L\rvert}$	Requires known labeling fraction; must avoid self-quenching for accurate quantification
Spectroscopy	IRRAS	IR reflectance-absorbance spectrum	Secondary structure of peptides	Vibrational modes of peptide bonds	Requires water-vapor corrections
			Orientation of lipids and peptides	Dichroic ratio, $\mathrm{R}=I_\parallel/I_\perp$	Polarization-dependent absorbance
			Lipid-peptide interactions	Vibrational modes of lipid-headgroups	Sensitive to hydrogen bonding and charge interactions
	NR	Intensity of reflected beam vs q_z	Composition, thickness and roughness hydration layers and interfacial water	Scattering length density profile modeling	Enables isotopic contrast (H/D); requires large facilities
	XR	Intensity of reflected beam and electron density profile perpendicular to the interface	Discretization of molecular layers	Fitting into an interface model of uniform slabs/layers of different thickness, density and roughness	On Langmuir-trough or possible beam artifacts; requires smooth monolayers. Highly sensitive to electron-density contrast
			Molecular aggregation (lipids/AMPs)		
			Peptide or water penetration		
	GIXD	Grazing-incidence diffraction pattern	Lateral packing and ordering (symmetry & chain tilt)	Number and position of Bragg peaks	Requires ordered phases
			Domain size and inhomogeneities	Scherrer formula using FWHM of Bragg peaks	Correlation length determination
			Tail group ordering	Bragg rod profile maximum values	Sensitive to chain tilt and ordering
	SFG	Visible + IR sum-frequency signal	Lipid-peptide interaction and hydrogen bonding rearrangement	Vibrational modes of lipid-headgroups	Surface-specific nonlinear technique
			Peptide conformation	Vibrational modes of peptides (amide I)	Distinguishes parallel vs perpendicular orientations
			Orientation of lipids and peptides	Vibrational modes using different polarization combinations	Requires careful phase-matching calibration
	FCS	Fluctuations in fluorescence intensity	Lateral difussion coefficient	Fluorescence intensity autocorrelation	Requires fluorescent labeling; sensitive to background and photophysics
			Binding/unbinding kinetics	2-state or multi-state kinetic models	Typical timescales from μs to s
	CD	Differential absorption of left- right- circularly polarized light	Secondary structure transitions	Ellipticity changes identified with each conformation	Requires transparent substrate; avoid scattering
			Degree of folding upon membrane binding	Spectral deconvolution	Bulk technique complements IRRAS/SFG for orientation

Table 3
Methods enabling quantitative determination of interfacial thermodynamics, mechanical response, and molecular-scale structure in AMP-perturbed lipid monolayers: comparison between experimental observables and MD-derived descriptors.

	Property	What is measured	Experimental	Computational
Interfacial Thermodynamics & Adsorption	Surface pressure (π)	Change in interfacial free energy	Langmuir isotherms	Interfacial tension from virial (NVT/NPAT/NPγT)
	Gibbs free energy of adsorption (ΔG_{ads})	Adsorption isotherm parameters (model dependent)	π–A shifts; fluorescence/IRRAS → Γ(c)	PMF (umbrella sampling/metadynamics/OPES), WHAM/MBAR
	Partitioning constant	Adsorbed vs bulk ratio	Fluorescence, IRRAS, radiolabel	Density profiles; depth PMF
Mechanical Response & Dynamics	Viscoelasticity	Shear/dilatational response	Interfacial rheology	Stress–relaxation, oscillatory perturbations
	Lateral diffusion	Mobility	FCS, FRAP	MSD, velocity autocorrelation function
Molecular Structure, Orientation & Disorder	Morphology/domains	Phase coexistence, domain structure	BAM, AFM, fluorescence	Order parameter clustering, density maps
	Peptide conformation	Secondary structure	CD, IRRAS, SFG	DSSP, helicity, α-RMSD
	Orientation	Tilt and alignment	IRRAS, GIXD, SFG	Tilt distributions, SCD parameters
	Lateral packing	2D crystalline order	GIXD	Voronoi tessellation, RDF
Layered Density, Thickness & Interface Structure	Penetration depth	Position along normal	NR/XRR (indirect)	z-density profiles, PMF minima
	Thickness	Film height	AFM, ellipsometry, NR/XRR	Density layering
	Molecular density profiles	Vertical distribution	NR/XRR	1D density profiles (water/lipid/peptide)

analysis by isolating the thermodynamic component of AMP binding and quantifying how interfacial packing governs adsorption energetics.

6.1.4. Surface potential measurements

Surface potential (ΔV) measurements quantify collective dipolar reorganizations at the air–water interface that may not produce strong signatures in π–A isotherms or in the compressibility modulus. The measured potential arises from the vector sum of all molecular dipoles contributing to the interfacial layer—including lipid headgroups, interfacial water, and the intrinsic dipole of the peptide. Recording ΔV–A isotherms therefore provides a sensitive probe of how AMPs perturb this dipolar architecture. From the maximum surface potential change at a given molecular area, the apparent normal dipole moment per molecule ($\mu_{\perp}^{A}$) can be estimated using:

$$\mu_{\perp}^{A} = \varepsilon_0 A \Delta V_{max}, \tag{7}$$

where A is the area per molecule and $\Delta V_{\max}$ is the maximum surface potential change. Although this relation is based on simplified dipole-layer models and neglects higher-order multipolar contributions, it offers a useful semiquantitative metric of how AMP binding modifies interfacial dipole density.

AMPs can influence ΔV in several ways: by reorienting lipid headgroups, by modifying the structure and orientation of the interfacial water layer, or by introducing their own dipole moment upon adsorption or partial insertion. Surface clustering or compression-induced ordering of peptides can enhance these effects, producing characteristic shifts in the ΔV–A profile. Importantly, such dipolar changes may occur even when π–A signatures remain subtle, making surface potential measurements particularly valuable for detecting early or partially reversible peptide-binding events.

When interpreted together with structural information from IRRAS or GIXD, ΔV–A curves help disentangle whether observed dipole changes originate from peptide orientation, lipid reorganization, or water restructuring. Thus, surface potential analysis complements the thermodynamic and mechanical observables described above by providing a distinct, dipole-resolved perspective on AMP–monolayer interactions.

6.2. Rheology methods

Rheological measurements complement the compressibility modulus by resolving the frequency-dependent mechanical response of monolayers. These experiments quantify dilatational and shear viscoelastic properties and reveal relaxation processes, dissipative rearrangements, and kinetic barriers that cannot be inferred from static π–A isotherms.

In the oscillating-barrier method, where an interfacial shear rheometer (ISR) is coupled to a Langmuir monolayer, the monolayer is held at a fixed surface pressure or molecular area while the barriers undergo sinusoidal oscillations of amplitude ΔA and frequency ω. Surface pressure is recorded using the Wilhelmy plate in two orthogonal orientations: parallel (∥) and perpendicular (⊥) to the barriers, yielding $\Delta\Pi_{\parallel}$ and $\Delta\Pi_{\perp}$. From these measurements, the dilatational modulus (E) and the shear modulus (G) are determined, both of which depend on ω and ΔA [123,124]. E quantifies the resistance to area changes (expansion/compression), whereas G describes the resistance to shape deformations at constant area. In the limit of very low frequencies, the dilatational modulus approaches the quasi-equilibrium compressibility modulus C_s^{-1}.

The viscoelastic behavior of the monolayer is characterized by the phase shift θ between area oscillation and surface-pressure response, given by:

$$\theta = 2\pi\omega\,\delta t$$

$$\widehat{A} = A_0/(2\Delta A)$$

where δt is the time delay between the imposed area oscillation and the pressure response, and Â is the reduced area amplitude. An in-phase response (θ = 0°) corresponds to a purely elastic monolayer, whereas a 90° phase lag indicates purely viscous behavior. Intermediate values reflect mixed viscoelasticity arising from molecular rearrangements, interfacial friction, or AMP-induced restructuring.

Operationally, the complex dilatational and shear moduli E*(ω) and G*(ω) are defined from the in-phase and out-of-phase components of the surface-pressure response with respect to the imposed area oscillation. Using the pressure amplitudes in the parallel and perpendicular configurations ($\Delta\Pi_{\parallel}$, $\Delta\Pi_{\perp}$) and the reduced area amplitude Â, the elastic (E′, G′) and viscous (E″, G″) components (real and imaginary contributions to E* and G*) are calculated according to:

$$E' = \widehat{A}\,(\Delta\Pi_{\parallel} + \Delta\Pi_{\perp})\cos\theta$$

$$G' = \widehat{A}(\Delta\Pi_{\parallel} - \Delta\Pi_{\perp})\cos\theta$$

$$E'' = \widehat{A}(\Delta\Pi_{\parallel} + \Delta\Pi_{\perp})\sin\theta$$

$$G'' = \widehat{A}(\Delta\Pi_{\parallel} - \Delta\Pi_{\perp})\sin\theta \tag{8}$$

the total moduli being $E = (E'^2 + E''^2)^{1/2}$ and $G = (G'^2 + G''^2)^{1/2}$. A purely

elastic monolayer ($E'' = G'' = 0$) exhibits zero hysteresis, whereas viscous or reorganizing monolayers show non-zero hysteresis energy during compression–expansion cycles [125].

The relaxation dynamics of the interface can be described by the characteristic frequency $\omega_R = \tau_R^{-1}$, which marks the crossover between elastic and viscous regimes. It relates to the low-frequency (E_L) and high-frequency (E_H) limits of the dilatational modulus through:

$$E(\omega) = \left[\frac{E_H^2 + \left(E_L^2 \omega_R^2\right)/\omega^2}{1 + \left(\omega_R^2\right)/\omega^2}\right]^{1/2} \quad (9)$$

Together, these rheological parameters provide a complete dynamic description of AMP-perturbed monolayers, revealing relaxation pathways and dissipative processes that are not accessible from π–A isotherms or the static compressibility modulus alone.

6.3. Spectroscopic analysis

Spectroscopic techniques provide essential molecular-level information that complements the thermodynamic and mechanical observables described above. They resolve secondary structure, orientation, hydration, interfacial hydrogen bonding, and peptide–lipid interactions with a level of detail that cannot be obtained from π–A isotherms, C_s^{-1}, or rheology alone. Together, these methods clarify how AMPs reorganize at the air–water interface, how they perturb lipid packing, and how interfacial water responds to peptide binding.

IRRAS is one of the most powerful techniques for characterizing peptide structure and orientation at the air–water interface [36,38,43,45–47,82,126]. By analyzing the amide I and II vibrational bands, IRRAS readily distinguishes α-helices (amide I at 1650–1660 cm^{-1}) from β-sheet structures (amide I at ~1620–1630 cm^{-1}). Polarization-dependent measurements enable determination of peptide orientation relative to the interface via dichroic ratios, while changes in headgroup vibrational modes, such as the phosphate symmetric stretching band near 1080 cm^{-1}, report on peptide–lipid interactions and hydrogen-bond rearrangements. IRRAS is particularly well suited to identifying compression-induced structural transitions and cooperative assembly of AMPs within monolayers.

XR [35,38,39,41,84] and neutron reflectivity (NR) [91,117] provide complementary insight into the vertical organization of AMP–lipid monolayers. XR yields electron-density profiles perpendicular to the interface, reporting on film thickness, peptide insertion depth, lipid hydration, and density fluctuations. NR offers subnanometer resolution of interfacial water layers and can exploit H/D contrast to isolate peptide, lipid, and water contributions. Both techniques reveal how AMPs alter monolayer compactness, promote water penetration, or induce multilayered structures. XR and NR excel at resolving out-of-plane structural rearrangements that accompany AMP insertion or aggregation.

GIXD [30,37–39,41,46] characterizes the lateral packing and crystalline order of lipid monolayers. The number, position, and width of Bragg peaks reflect hydrocarbon-chain tilt, symmetry, and domain size, providing a direct measurement of how AMPs perturb lateral organization. Peptide-induced fluidization, disruption of condensed lipid phases, or stabilization of particular packing motifs can be identified from shifts in peak positions and from reductions in the in-plane correlation length, extracted via the Scherrer relation. GIXD is therefore uniquely sensitive to peptide-induced changes in lateral ordering, effects that often remain hidden in π–A isotherms.

Sum frequency generation (SFG) spectroscopy [127–131], a surface-specific nonlinear optical technique, probes vibrational modes of lipids and peptides at the interface. Because SFG is forbidden in centrosymmetric media, it selectively detects ordered interfacial species. In AMP–lipid monolayers, SFG resolves headgroup orientation, hydrogen-bond reorganization, and peptide secondary-structure signatures in the amide I region. Through different polarization combinations, SFG provides orientational information that complements IRRAS and reveals subtle interfacial ordering events triggered by peptide adsorption, even at low surface coverages where other techniques are less sensitive.

CD spectroscopy [127–129,132] is often used to monitor AMP secondary structure, though it typically requires immobilizing peptides on solid-supported self-assembled monolayers (SAMs) or measuring bulk peptide–lipid mixtures. CD excels at detecting α-helix to β-sheet transitions upon membrane interaction, but lacks the interfacial specificity of IRRAS or SFG. Still, it provides valuable information on structural changes accompanying AMP aggregation or membrane binding.

Fluorescence correlation spectroscopy (FCS) [133] probes lateral diffusion and adsorption–desorption kinetics by analyzing temporal fluctuations in fluorescence intensity. In AMP-containing monolayers or SAM-supported films, FCS quantifies peptide diffusion coefficients, partitioning behavior, and residence times at the interface. Partitioning constants can be extracted from fluorescence lifetimes using Eq. 10 [134], providing an independent assessment of AMP affinity that complements Gibbs adsorption analysis.

$$\tau = \frac{\tau_W + Kx_L|L|\tau_L}{1 + Kx_L|L|} \quad (10)$$

where τ, τ_W, τ_L denote the average fluorescence lifetime measured, for the peptide in bulk and for the peptide in the monolayer, respectively, x_L is the lipid molar volume and $|L|$ the lipid concentration.

Together, spectroscopic approaches reveal how AMPs reorganize at the air–water interface across multiple length scales: IRRAS and SFG resolve structure and orientation; XR and NR characterize vertical organization and hydration; GIXD captures lateral packing and domain integrity; and FCS quantifies interfacial dynamics. Despite their strengths, some methods (such as GIXD or NR) require synchrotron or neutron sources, and disordered or highly aggregated states can challenge structural interpretation. Nonetheless, spectroscopy provides indispensable molecular insight that, when combined with microscopy and mechanical measurements, yields a comprehensive framework for understanding AMP–monolayer interactions.

6.4. Microscopy methods

Microscopy techniques provide direct spatial visualization of AMP-containing monolayers and reveal mesoscale and nanoscale organization that cannot be accessed through isotherms, rheology, or spectroscopy alone. These methods resolve domain formation, lateral heterogeneity, peptide aggregation, and structural rearrangements induced by AMP binding at the air–water interface.

BAM [29,30,32,43,46,87,135] is a non-invasive optical method that enables real-time imaging of monolayers directly on the Langmuir trough. Because p-polarized light exhibits minimal reflectance at the Brewster angle for pure water, contrast arises exclusively from interfacial films. BAM is therefore highly effective at visualizing mesoscale morphology, including the formation, growth, and disruption of condensed lipid domains [32,46,87,135]; AMP-induced fluidized regions [29,43]; peptide clusters [29,30]; and collapse or "squeeze-out" events at high surface pressures. In lipid-free peptide films, AMPs typically spread homogeneously at low pressures but form bright domains as compression promotes peptide aggregation [29,32,38,46]. In AMP–lipid mixtures, BAM readily reveals lipid-dependent effects such as the disruption of condensed DPPC phases or enhanced fluidization in anionic DPPG monolayers. Although BAM excels at mesoscale imaging and dynamics during compression-expansion cycling, it is limited by a lateral resolution of ~1 μm and cannot resolve molecular-scale features or determine molecular orientation.

Atomic force microscopy (AFM) [29,30,135,136] provides nanoscale structural information after transferring the monolayer onto a solid substrate, typically via the Langmuir–Blodgett method. AFM resolves topography, domain boundaries, peptide aggregates, holes, and

roughness with nanometer precision. In AMP–lipid monolayers, AFM reveals disruption of condensed phases, peptide accumulation at domain edges, and changes in film thickness or packing. It is particularly useful for assessing nanoscale consequences of peptide insertion or aggregation that are not visible in BAM. Specifically, BAM offers a lateral resolution of approximately 1 μm. This defines the threshold for detecting peptide-induced domains or clusters; features smaller than this limit require the nanometric precision of AFM, which resolves topography and domain boundaries at the sub-micrometer scale after monolayer transfer. However, because AFM requires monolayer transfer, artifacts related to drying, substrate interactions, or transfer-induced rearrangements may arise, and dynamic interfacial processes cannot be captured.

Fluorescence microscopy, and in particular epifluorescence, is widely employed to characterize AMP–lipid monolayers at the air–water interface, providing spatially resolved insight into molecular organization, phase behavior, and lateral dynamics [29,32,43,46]. By labeling AMPs or lipid components with fluorescent probes, this method enables visualization of domain formation within the monolayer, including lipid phase separation (e.g., liquid-expanded vs. liquid-condensed phases) and AMP-induced disruption of lipid packing [43,137]. Additionally, it can monitor peptide aggregation, adsorption, or exclusion from the monolayer under varying surface pressures or molecular densities [29,138], thereby revealing whether AMPs preferentially partition into specific phases or are expelled from ordered regions. Under appropriate calibration, fluorescence intensity ratios and fluorescence lifetime analysis can be used to estimate peptide partitioning between coexisting phases, providing a qualitative or semi-quantitative view of AMP affinity that complements the more rigorous thermodynamic treatment discussed in Section 6.3. Epifluorescence is particularly useful for assessing miscibility and interactions in mixed peptide–lipid films and for identifying peptide localization in more hydrophilic versus more hydrophobic regions. However, these methods rely on fluorescent labels, which may perturb AMP or lipid properties, and are susceptible to photobleaching and self-quenching, so careful control experiments are required.

Transmission electron microscopy (TEM) [139–141] provides ultrastructural imaging of AMP-induced deformations in lipid assemblies derived from monolayers, such as vesicles, collapsed films, or multilayered aggregates formed during compression or upon transfer. TEM has directly visualized vesicle collapse, pore-like defects, and severe structural disintegration caused by AMPs, offering high spatial resolution insights into their disruptive mechanisms. A major limitation is the relatively complex sample preparation often involving freeze-fracture, staining, or drying, which can introduce artifacts and precludes real-time observation at the air–water interface.

Microscopy techniques collectively reveal critical aspects of AMP behavior at interfaces. BAM and fluorescence microscopy excel in capturing mesoscale dynamics, domain transitions, and peptide partitioning, while AFM and TEM provide nanoscale details of aggregation, roughness, and structural deformations. Together, these methods complement thermodynamic, mechanical, and spectroscopic analyses, providing an integrated framework to understand AMP interfacial organization and antimicrobial activity.

6.5. Computational approaches: from atomistic interactions to mesoscale modeling

Computational methods, particularly MD simulations, play a crucial role in advancing the understanding of AMP–lipid monolayers by providing atomic- to mesoscale insight into thermodynamic properties, structural organization, and aggregation mechanisms that are often elusive to experimental probes (Table 3). Rather than merely reproducing experimental data, modern simulations serve to deconstruct the driving forces of peptide adsorption, offering a *computational microscope* to visualize hydrogen bonding networks, hydrophobic contacts, and dynamic lipid remodeling.

6.5.1. Atomistic simulations, thermodynamics, and experimental validation

All-atom (AA) MD simulations offer high-resolution information on molecular interactions, capturing the precise interplay between peptide side chains, lipid headgroups, and interfacial water. A critical challenge in these simulations is the accurate determination of surface tension (γ) to match specific experimental states of compression (LE vs LC phases). The choice of lipid force fields and water models significantly influences the calculated γ, which is computed from the pressure tensor components. In MD, γ is typically computed from the pressure tensor components as:

$$\gamma = \frac{L_z}{2}\left[P_{zz} - \frac{P_{xx} + P_{yy}}{2}\right] \tag{11}$$

where L_z is the length of the simulation box perpendicular to the monolayer and P_{ii} are the diagonal components of the pressure tensor. Recent benchmarking has shown that standard three-point water models may underestimate interfacial tension; thus, the integration of four-point models (e.g., OPC) [142] with modern additive force fields like CHARMM36m [143] has improved the quantitative agreement with Langmuir isotherms by better capturing the lipid–water interaction energetics [144]. Inaccurate parameterization of these interfacial forces can lead to significant deviations in the predicted phase behavior, potentially over-stabilizing condensed phases and misinterpreting the peptide's disruptive capacity.

The synergy between simulations and experiments extends to structural validation. For instance, MD has been used to interpret NR profiles. McCluskey et al. demonstrated that while all-atom (Slipid) and united-atom (Berger) models reproduced experimental reflectivity curves well, coarse-grained (MARTINI) models struggled to capture quantitative details due to the loss of atomistic roughness, highlighting the need for careful model selection when validating against scattering data [145].

6.5.2. Dynamics, structural order, and sampling

Beyond thermodynamics, MD provides unique access to dynamic and structural properties. Lateral diffusion is commonly extracted from the mean square displacement (MSD) of lipid centers of mass:

$$\langle |\mathrm{r}(\mathrm{t}_2) - \mathrm{r}(\mathrm{t}_1)|^2 \rangle = 4\,\mathrm{D}\,\Delta\mathrm{t} \tag{12}$$

where $\mathrm{t}_2 - \mathrm{t}_1 = \Delta\mathrm{t}$ is the time interval and r(t) is the position of the lipid center of mass at time t. The resulting diffusion coefficient D allows for direct comparison with FCS data. Structurally, the effect of AMPs on lipid packing is quantified by the lipid chain order parameter (S_{CH}):

$$S_{CH} = \tfrac{1}{2}\left\langle 3\cos^2\theta - 1 \right\rangle \tag{13}$$

where θ is the angle between a given C—H bond vector and the normal to the monolayer plane, and the brackets denote averaging over time and over all relevant lipids in the simulation box. Profiles of S_{CH} distinguish between disordered (LE) and ordered (LC) state [146]. Additionally, radial distribution functions, $g(r)$, and cluster analysis are frequently used to characterize lipid heterogeneity and domain formation.

However, AA-MD is computationally expensive. To overcome energy barriers and sample rare events—such as peptide folding or deep insertion—advanced sampling techniques like Replica Exchange MD (REMD) [147], Accelerated MD (aMD) [148], or High-Temperature MD (HT-MD) [149,150] are increasingly employed to flatten energy landscapes and accelerate kinetics.

6.5.3. Bridging scales: hierarchical multiscale modeling

To investigate large-scale phenomena such as domain formation or pore nucleation, which occur on timescales (milliseconds) and length scales (micrometers) beyond atomistic reach, hierarchical (or sequential) multiscale modeling has emerged as the robust standard in

membrane biophysics. In this approach, finer-scale atomistic simulations are used to parameterize or validate Coarse-Grained (CG) models, such as those based on the MARTINI force field [151].

CG-MD groups atoms into effective beads to reduce degrees of freedom, enabling the simulation of cooperative phenomena like the *carpet* mechanism or lipid-mediated peptide aggregation. However, the interpretation of monolayer behavior through CG models requires caution; the "bead" parameterization inherently smooths out the atomistic roughness of the interface, which can lead to discrepancies when validating against high-resolution scattering data such as NR or GIXD. While CG-MD excels at capturing mesoscale cooperative events like pore nucleation, AA simulations remain necessary to resolve the specific side-chain orientations and dipolar reorganizations that drive experimental surface potential shifts. Bridging these scales through hierarchical modeling allows for a more robust interpretation of how molecular-level interactions propagate into macroscopic monolayer remodeling. Complementary to these simulations, sequence-based prediction tools such as *AGGRESCAN* [152] and *TANGO* [153] provide rapid estimates of aggregation-prone regions, which can help interpret the peptide clustering observed in CG trajectories. However, it is important to note a gap in the current literature: while this hierarchical strategy has been extensively applied to AMP interactions with lipid bilayers [154,155] and lung surfactant monolayers [156,157] its application to AMP interactions with lipid monolayers at the air–water interface remains limited. Consequently, extending hierarchical multiscale protocols to these specific interfacial systems represents a significant opportunity for future research to quantitatively link the mesoscale domain morphologies observed in microscopy (e.g. BAM) with molecular-level peptide organization.

6.5.4. Software ecosystem and future challenges

A wide ecosystem supports these studies. *CHARMM-GUI* [158,159] facilitates the construction of complex monolayer systems. Simulation engines include *GROMACS* [160], *LAMMPS* [161], *AMBER* [162], *OpenMM* [163], *CHARMM* [164] and *NAMD* [165]. Post-processing is handled by libraries like *MDAnalysis* [166] and specialized tools such as LiPyphilic [167], *Pytim* [168], or *SuAVE* [169]. To ensure reproducibility, the community relies on curated databases like *LipidBook* [170] and *NMRlipids* [171].

Despite these advances, challenges remain. Enhanced parameterization for AMP-specific properties in CG models is critical, as is better accounting for experimental variables like pH and ionic strength. Looking forward, the integration of Artificial Intelligence (AI) to analyze trajectory datasets [172–174] and exploratory studies using quantum computing to simulate folding at interfaces [175] promise to move the field from descriptive phenomenology to rational peptide design.

7. Case studies: integrative insights into AMP-monolayer interactions

Experimental and computational investigations of AMPs at interfaces provide critical insights into the thermodynamic driving forces (e.g., insertion free energy), dynamic behavior (e.g., penetration depth, aggregation), and structural consequences (e.g., phase separation, fluidization) of peptide–membrane interactions. Rather than viewing these studies in isolation, a comparative analysis reveals common mechanistic trends governed by the interplay between peptide amphiphilicity and lipid packing. Table 4 summarizes key representative studies, highlighting the methodologies used and the biophysical principles established.

7.1. Intrinsic interfacial behavior: self-assembly and structural stability

Before interacting with lipids, AMPs must access the air–water interface, a process that is connected to their intrinsic amphiphilicity and folding propensity. Studies on peptides like SMAP-29 and LL-37 fragments demonstrate that the air–water interface acts as a template for secondary structure induction. For instance, XR analysis of SMAP-29 reveals a *two-slab* electron density profile, indicating a specific orientation where hydrophobic residues face the air while hydrophilic residues remain hydrated, although GIXD suggests these films lack long-range crystalline order [84]. Similarly, the stability of these films is size-dependent: while the longer LL-32 fragment forms robust α-helical monolayers capable of sustaining high surface pressures (24 mN/m), the shorter LL-20 fragment forms heterogeneous, less stable films, highlighting the critical role of sequence length in interfacial stabilization [176].

The dynamic response to compression provides further insight into aggregation mechanisms. Research on dicynthaurin shows that while both monomers and dimers form stable monolayers, high compression forces lead to irreversible material loss (*squeeze-out*) into the subphase, a behavior indicative of a kinetic barrier to re-adsorption [46]. This sensitivity to amphiphilic balance was systematically explored using synthetic peptide analogs. It was observed that analogs with distinct hydrophilic-lipophilic balances exhibit different vertical positioning: non-polar analogs remain at the water-vacuum interface, while balanced analogs penetrate deeper into the water subphase. Furthermore, compression isotherms of these analogs reveal varying degrees of hysteresis, underscoring how subtle sequence variations alter the thermodynamic stability and reversibility of the monolayer [177]. While MD simulations have attempted to model these intrinsic behaviors, capturing the full complexity of these rearrangements remains challenging due to timescale limitations and force field accuracy.

Table 4
Representative case studies of AMP interactions with Langmuir monolayers, highlighting key methodological approaches and mechanistic insights.

Peptide Family	Lipid System	Key Methodologies	Main Biophysical Finding	Ref.
SMAP-29	Air-water / DPPG / DPPC	Langmuir, XR, GIXD	At Air-Water: Forms stable amphipathic films with a two-slab electron density profile but lacks long-range crystalline order. With Lipids: Exhibits high affinity for anionic DPPG while showing weaker interaction with zwitterionic DPPC (see section 4.1).	[84]
LL-37 & fragments	DPPG, DPPC, DPPE, *L. gormanii* lipids	Langmuir, BAM, GIXD, IRRAS	*Carpet* mechanism. Inserts into and fluidizes anionic monolayers (DPPG, CL). Excluded from zwitterionic (DPPC) and tightly packed (DPPE) films. Helical stability depends on chain length (LL−32⟩ LL-20).	[36,88,137,176]
Arenicin-1	DPPG vs DPPC	Langmuir, IRRAS, GIXD	Fluidizes anionic hydrocarbon chains (increased *gauche* defects). Electrostatic attraction drives partial penetration; hydrophobic mismatch drives disruption. Excluded from DPPC at high π.	[37]
Dicynthaurin	Air-water (Lipid-free)	Langmuir cycles	Forms stable monolayers up to high pressures (~30 mN/m). Compression induces irreversible aggregation (squeeze-out), indicating kinetic barriers to re-adsorption.	[46]
Synthetic $(KX)_4K$	DMPA, DMPG, TMCL	Langmuir, Fluorescence	Hydrophobicity controls insertion depth; charge controls initial binding. Lipid headgroup size modulates domain morphology (e.g., filamentous domains in DMPA due to reduced line tension).	[43]
Synthetic Amphipathic Analogs	Air-water (lipid free)	Langmuir, MD	The hydrophilic/lipophilic balance governs the vertical positioning of the peptide: non-polar analogs remain at the air interface, while balanced analogs penetrate deeper into the subphase.	[177]

7.2. Lipid selectivity and membrane remodeling

When lipids are introduced, the interaction landscape is dominated by the interplay between electrostatic attraction and hydrophobic insertion. A universal trend observed across multiple AMP families—including LL-37, Arenicins, and SMAP-29—is the stark discrimination between anionic and zwitterionic lipids (Fig. 7).

7.2.1. Electrostatic targeting and insertion

In anionic monolayers (e.g., DPPG, Cardiolipin), cationic AMPs typically induce a significant expansion of molecular area and a fluidization of the acyl chains. For example, LL-37 has been shown to disrupt the condensed phase of DPPG, effectively *melting* the ordered domains into a fluid state, a process consistent with a *carpet* mechanism of disruption [137]. This interaction is thermodynamically favorable, as evidenced by negative Gibbs energies of mixing. Specifically, Langmuir studies indicate that AMP insertion and interfacial reorganization are optimal at intermediate surface pressures, where lipid fluidity allows for peptide accommodation without the steric hindrance observed in highly condensed phases [30,46]. In contrast, zwitterionic monolayers (e.g., DPPC, DPPE) often show positive mixing energies and phase separation, where the peptide is excluded from the lipid lattice at physiologically relevant surface pressures (>30 mN/m) [37,88].

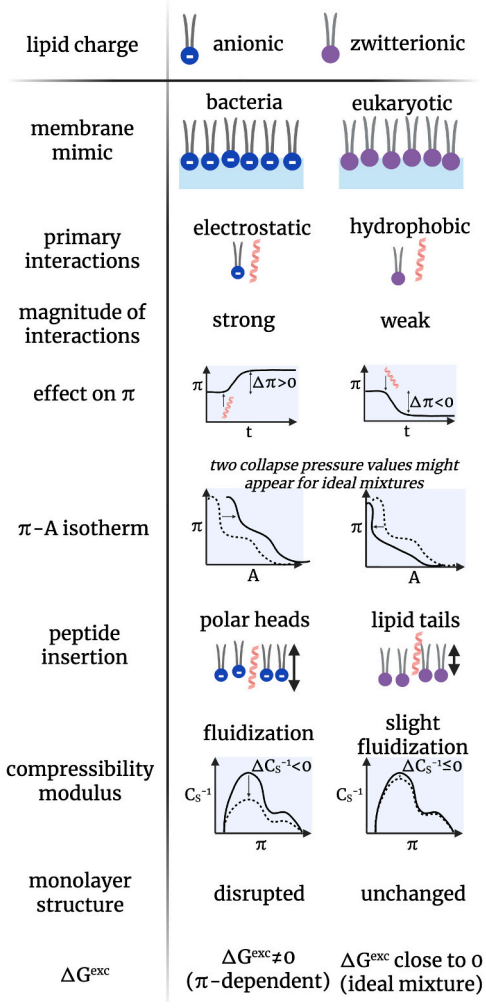

Fig. 7. Scheme of the general trends that follows AMP adsorption to lipid monolayers depending on lipid charge (mimicking different cell membrane models).

7.2.2. Hydrophobic mismatch and domain morphology

Beyond simple charge attraction, the hydrophobic match between the peptide and the lipid tails dictates the extent of disruption. Studies using synthetic $(KX)_4K$ peptides revealed that increasing the hydrophobicity of the peptide side chains shifts the liquid-expanded to liquid-condensed (LE-LC) phase transition to higher pressures, effectively stabilizing the fluid phase. Interestingly, the geometry of the lipid headgroup also plays a role: peptides interacting with small-headgroup lipids (like DMPA) reduced the line tension at domain boundaries, leading to the formation of exotic filamentous domain shapes observed by fluorescence microscopy [43].

7.2.3. Structural perturbations

At the molecular level, these macroscopic changes correspond to a loss of lipid order. IRRAS and GIXD measurements on Arenicin-containing monolayers confirmed an increase in *gauche* conformers within the hydrocarbon chains, directly quantifying the *disordering* effect of the peptide. However, an interesting counter-effect is observed in some strongly interacting systems (like DPPG), where the electrostatic *pinning* of the headgroups by the peptide can locally induce a more upright chain orientation before the eventual collapse of the monolayer structure [37].

Collectively, these case studies demonstrate that Langmuir monolayers allow for the decoupling of key variables—charge, saturation, and headgroup geometry—providing a mechanistic map of how AMPs transition from surface adsorption to membrane disruption.

8. Challenges and future directions in AMP-lipid monolayer studies

The study of AMPs interacting with lipid monolayers has provided valuable insights into their mechanisms of action, including membrane disruption, selective targeting, and potential therapeutic applications. Lipid monolayers serve as simplified yet powerful models that allow for the precise investigation of peptide-lipid interactions under controlled conditions. However, despite significant advancements, several challenges remain that must be addressed to fully harness the potential of AMP-lipid monolayer studies for both fundamental research and practical applications.

8.1. Experimental challenges and standardization

One of the major challenges in AMP-lipid monolayer studies is the lack of standardization in experimental conditions. Variations in subphase composition (e.g., pH, ionic strength, and buffer type), lipid purity, and peptide preparation methods introduce inconsistencies across studies, making direct comparisons difficult. Additionally, the influence of external parameters such as temperature, surface pressure, and lipid packing density can lead to divergent results, complicating the interpretation of peptide-membrane interactions. Standardized experimental protocols, including the use of well-characterized lipids and peptides under reproducible conditions, are essential to ensure comparability and reliability of findings.

Another experimental limitation is the inherent complexity of biological membranes, which often contain heterogeneous lipid mixtures, asymmetry, and dynamic remodeling that are not fully captured by monolayer models. While monolayers provide a controlled environment, they lack features such as bilayer curvature, transmembrane asymmetry, and lipid-protein interactions, which are crucial for accurately replicating biological membranes. Future efforts should focus on combining monolayers with other model systems, such as supported lipid bilayers or vesicles, to provide a more comprehensive picture of AMP antimicrobial activity.

Furthermore, time-dependent phenomena, such as peptide adsorption kinetics, membrane insertion, and lipid domain reorganization, remain difficult to assess with traditional Langmuir trough techniques.

Real-time, high-resolution imaging methods, such as BAM and fluorescence microscopy, can provide valuable insights but are limited by spatial resolution and contrast issues. Developing integrated experimental platforms that combine multiple characterization techniques (e.g., Langmuir trough coupled with infrared spectroscopy or X-ray reflectivity) could enhance our understanding of AMP dynamics in lipid monolayers.

8.2. Limitations of current analytical techniques

Despite the availability of advanced surface-sensitive techniques, several analytical challenges persist in AMP-lipid monolayer studies. Techniques such as GIXD and IRRAS provide critical information about peptide orientation and lipid order, but they require specialized facilities and complex data interpretation. Additionally, current methods may struggle to capture subtle structural transitions, such as peptide-induced lipid phase separation or transient pore formation, which are essential for understanding AMP mechanisms.

Another significant limitation is the difficulty in resolving interfacial water structure and its impact on AMP-lipid interactions. Hydration forces and hydrogen bonding play crucial roles in AMP adsorption and membrane destabilization, yet these effects are challenging to probe experimentally. Neutron reflectometry and SFG spectroscopy hold promise for studying these interactions in greater detail but are currently underutilized in AMP-lipid monolayer research.

8.3. Computational modeling and theoretical challenges

Computational simulations offer powerful tools to complement experimental studies, providing atomic-level insights into AMP-lipid interactions. However, several limitations hinder their full potential. All-atom MD simulations, while highly detailed, are computationally expensive and often limited to short timescales (nanoseconds to microseconds), which may not capture long-term peptide insertion or lipid reorganization dynamics. Coarse-grained models, such as those using the MARTINI force field, allow for longer timescales but sacrifice atomic-level precision, potentially oversimplifying peptide-lipid interactions.

A critical challenge in computational modeling is the accurate parameterization of lipid and peptide force fields, ensuring compatibility and reproducibility across different simulation platforms. Recent efforts, such as the integration of lipid-specific force fields from databases like LipidBook or Charmmgui, have improved the accuracy of lipid simulations, but further refinement is needed to capture the full complexity of AMP-induced membrane disruption. Additionally, the development of hybrid multiscale modeling approaches, which integrate atomistic and coarse-grained simulations, could provide a more comprehensive understanding of AMP-lipid interactions across different scales.

The use of artificial intelligence presents another transformative opportunity in this field. Machine learning algorithms can analyze large datasets simultaneously considering multiple features from experiments and simulations, identifying patterns and correlations that might be overlooked by conventional methods [173,174]. AI-driven approaches could accelerate the design of AMP-based applications by predicting optimal peptide sequences or experimental conditions for desired properties [172]. Similarly, AI could enhance the characterization of monolayers by integrating diverse data types, such as π-A isotherms, spectroscopic profiles, and simulation outputs, to generate comprehensive insights into AMP behavior.

8.4. Toward more physiologically relevant model systems

While lipid monolayers provide valuable mechanistic insights, their translation to biologically relevant systems remains a challenge. The simplified nature of monolayers does not fully capture the complexity of cell membranes, which contain diverse lipid compositions, membrane proteins, and dynamic structural heterogeneity. Consequently, future studies should focus on integrative experimental frameworks that combine lipid monolayers (as outer leaflet mimetics) with bilayer systems (e.g., vesicles or supported bilayers). This combination allows researchers to decouple interfacial phenomena—such as initial peptide adsorption and lateral packing effects—from transmembrane processes like pore formation, thereby bridging the gap between simplified monolayers and complex biological membranes.

Additionally, incorporating membrane-mimicking lipid mixtures, including bacterial and eukaryotic lipid compositions, could provide more physiologically relevant models. The use of natural lipid extracts from pathogens or host cells can offer insights into how AMP selectivity and antimicrobial activity vary in different cellular environments. Further advancements in lipidomics will aid in the precise formulation of biomimetic models that better replicate the lipid diversity found in real membranes.

8.5. Expanding applications and future opportunities

Despite existing challenges, AMP-lipid monolayer studies hold significant promise for various applications beyond antimicrobial research. The ability of AMPs to modulate lipid organization and phase behavior presents opportunities for biotechnological and biomedical applications, such as antimicrobial coatings for medical devices, biosensing platforms, and targeted drug delivery systems. AMP-functionalized lipid monolayers could be employed in biosensors, leveraging their selective interactions with microbial membranes to enable rapid detection of pathogens.

In the context of AMR, AMP-lipid monolayer studies can inform the development of synergistic therapies, combining AMPs with conventional antibiotics or nanomaterials to enhance efficacy and reduce resistance development. Additionally, the exploration of AMP-lipid interactions in non-antimicrobial contexts, such as immunomodulation and wound healing, could broaden their therapeutic potential.

Finally, addressing regulatory and translational challenges will be essential for the successful integration of AMP-based technologies into clinical and industrial settings. Evaluating AMP stability, biocompatibility, and environmental impact remains critical to ensure their safe and effective application.

Declaration of AI and AI-assisted technologies in the writing process

During the preparation of this work the authors used ChatGPT (OpenAI, GPT-5) in order to improve language and readability. After using this tool/service, the authors reviewed and edited the content as needed and take full responsibility for the content of the publication.

CRediT authorship contribution statement

Paula Antelo-Riveiro: Writing – review & editing, Writing – original draft, Validation, Methodology, Investigation, Formal analysis, Data curation. **Rebeca Garcia-Fandino:** Writing – review & editing, Writing – original draft, Validation, Supervision, Resources, Project administration, Methodology, Investigation, Funding acquisition, Conceptualization. **Ángel Piñeiro:** Writing – review & editing, Writing – original draft, Validation, Supervision, Resources, Project administration, Methodology, Funding acquisition, Conceptualization.

Declaration of competing interest

The authors declare that they have no known competing financial interests or personal relationships that could have appeared to influence the work reported in this paper.

Acknowledgments

This work was supported by the Spanish Agencia Estatal de Investigación (AEI) and the ERDF (PID2022-141534OB-I00 and CNS2023-144353), by Xunta de Galicia (ED431C 2025/15, ED431C 2021/21 and Centro de investigación do Sistema universitario de Galicia accreditation 2023-2027, ED431G 2023/03) and the European Union (European Regional Development Fund – ERDF). P.A-R. thanks Xunta de Galicia for her predoctoral contract (ED481A-2024-073).

Data availability

No data was used for the research described in the article.

References

[1] Khanda M, Seal P, Mohan AJ, Arya N, Boda SK. Antimicrobial peptides and their application to combat implant-associated infections – opportunities and challenges. Nanoscale 2025;17:10462–84. https://doi.org/10.1039/D5NR00953G.
[2] Wang Y, Cong H, Shen Y, Yu B. Advances in the discovery, mechanism of action, optimization of activity and potential for clinical application of antimicrobial peptides. Chem Eng J 2025;504:158962. https://doi.org/10.1016/J.CEJ.2024.158962.
[3] Răileanu M, Borlan R, Campu A, Janosi L, Turcu I, Focsan M, et al. No country for old antibiotics! Antimicrobial peptides (AMPs) as next-generation treatment for skin and soft tissue infection. Int J Pharm 2023;642:123169. https://doi.org/10.1016/J.IJPHARM.2023.123169.
[4] Xuan J, Feng W, Wang J, Wang R, Zhang B, Bo L, et al. Antimicrobial peptides for combating drug-resistant bacterial infections. Drug Resist Updat 2023;68:100954. https://doi.org/10.1016/J.DRUP.2023.100954.
[5] Bucataru C, Ciobanasu C. Antimicrobial peptides: opportunities and challenges in overcoming resistance. Microbiol Res 2024;286:127822. https://doi.org/10.1016/J.MICRES.2024.127822.
[6] Ali M, Garg A, Srivastava A, Arora PK. The role of antimicrobial peptides in overcoming antibiotic resistance. Microbe 2025;7:100337. https://doi.org/10.1016/J.MICROB.2025.100337.
[7] Qu B, Yuan J, Liu X, Zhang S, Ma X, Lu L. Anticancer activities of natural antimicrobial peptides from animals. Front Microbiol 2024;14. https://doi.org/10.3389/FMICB.2023.1321386.
[8] Zare-Zardini H, Saberian E, Jenča A, Ghanipour-Meybodi R, Petrášová A, Jenčová J. From defense to offense: antimicrobial peptides as promising therapeutics for cancer. Front Oncol 2024;14. https://doi.org/10.3389/FONC.2024.1463088.
[9] Lamb HO, Benfield AH, Henriques ST. Peptides as innovative strategies to combat drug resistance in cancer therapy. Drug Discov Today 2024;29:104206. https://doi.org/10.1016/J.DRUDIS.2024.104206.
[10] Hanson MA, Lemaitre B. Antimicrobial peptides do not directly contribute to aging in Drosophila, but improve lifespan by preventing dysbiosis. DMM Disease Models Mech 2023;16. https://doi.org/10.1242/DMM.049965/307300.
[11] Stuart BAR, Franitza AL. Regulatory roles of antimicrobial peptides in the nervous system: implications for neuronal aging. Front Cell Neurosci 2022;16:843790. https://doi.org/10.3389/FNCEL.2022.843790/FULL.
[12] Conde-Torres D, Blanco-González A, Seco-González A, Suárez-Lestón F, Cabezón A, Antelo-Riveiro P, et al. Unraveling lipid and inflammation interplay in cancer, aging and infection for novel theranostic approaches. Front Immunol 2024;15:1320779. https://doi.org/10.3389/FIMMU.2024.1320779/FULL.
[13] Lee S, Silverman N, Gao FB. Emerging roles of antimicrobial peptides in innate immunity, neuronal function, and neurodegeneration. Trends Neurosci 2024;47:949–61. https://doi.org/10.1016/j.tins.2024.09.001.
[14] Mangoni ML, Mcdermott AM, Zasloff M. Antimicrobial peptides and wound healing: biological and therapeutic considerations. Exp Dermatol 2016;25:167–73. https://doi.org/10.1111/EXD.12929;ISSUE:ISSUE:DOI.
[15] Tripathi AK, Singh J, Trivedi R, Ranade P. Shaping the future of antimicrobial therapy: harnessing the power of antimicrobial peptides in biomedical applications. J Funct Biomater 2023;14:539. https://doi.org/10.3390/JFB14110539.
[16] Dennison SR, Morton LHG, Harris F, Phoenix DA. The impact of membrane lipid composition on antimicrobial function of an α-helical peptide. Chem Phys Lipids 2008;151:92–102. https://doi.org/10.1016/J.CHEMPHYSLIP.2007.10.007.
[17] Sani M-A, Whitwell T, Gehman JD, Separovic F. Antimicrobial peptide activity in a competitive membrane lipid environment. Biophys J 2013;104:20a–1a. https://doi.org/10.1016/j.bpj.2012.11.151.
[18] Sohlenkamp C, Geiger O. Bacterial membrane lipids: diversity in structures and pathways. FEMS Microbiol Rev 2016;40:133–59. https://doi.org/10.1093/FEMSRE/FUV008.
[19] Cockcroft S. Mammalian lipids: structure, synthesis and function. Essays Biochem 2021;65:813–45. https://doi.org/10.1042/EBC20200067.
[20] Zeng Q, Gong Y, Zhu N, Shi Y, Zhang C, Qin L. Lipids and lipid metabolism in cellular senescence: emerging targets for age-related diseases. Ageing Res Rev 2024;97:102294. https://doi.org/10.1016/J.ARR.2024.102294.
[21] Szlasa W, Zendran I, Zalesińska A, Tarek M, Kulbacka J. Lipid composition of the cancer cell membrane. J Bioenerget Biomembr 2020;52(5):321–42. https://doi.org/10.1007/S10863-020-09846-4.
[22] Nguyen LT, Haney EF, Vogel HJ. The expanding scope of antimicrobial peptide structures and their modes of action. Trends Biotechnol 2011;29:464–72. https://doi.org/10.1016/J.TIBTECH.2011.05.001.
[23] Dingjan T, Futerman AH. The fine-tuning of cell membrane lipid bilayers accentuates their compositional complexity. BioEssays 2021;43:2100021. https://doi.org/10.1002/BIES.202100021;ISSUE:ISSUE:DOI.
[24] Luchini A, Vitiello G. Mimicking the mammalian plasma membrane: an overview of lipid membrane models for biophysical studies. Biomimetics 2021;6:3. https://doi.org/10.3390/BIOMIMETICS6010003.
[25] Hollmann A, Martinez M, Maturana P, Semorile LC, Maffia PC. Antimicrobial peptides: interaction with model and biological membranes and synergism with chemical antibiotics. Front Chem 2018;6:363805. https://doi.org/10.3389/FCHEM.2018.00204/EPUB.
[26] Nisticò N, Greco M, Bruno MC, Giuliano E, Sinopoli P, Cosco D. Biomimetic lipid membranes: an overview on their properties and applications. Appl Mater Today 2023;35:101998. https://doi.org/10.1016/J.APMT.2023.101998.
[27] Guo X, Briscoe WH. Molecular interactions, elastic properties, and nanostructure of Langmuir bacterial-lipid monolayers: towards solving the mystery in bacterial membrane asymmetry. Curr Opin Colloid Interface Sci 2023;67:101731. https://doi.org/10.1016/J.COCIS.2023.101731.
[28] Ma X, Wang Q, Ren K, Xu T, Zhang Z, Xu M, et al. A review of antimicrobial peptides: structure, mechanism of action, and molecular optimization strategies. Fermentation 2024;10:540. https://doi.org/10.3390/FERMENTATION10110540.
[29] Krishnaswamy R, Rathee V, Sood AK. Aggregation of a peptide antibiotic alamethicin at the air−water interface and its influence on the viscoelasticity of phospholipid monolayers. Langmuir 2008;24:11770–7. https://doi.org/10.1021/LA8019765.
[30] Ionov R, El-Abed A, Goldmann M, Peretti P. Structural organization of α-helical peptide antibiotic alamethicin at the air/water Interface. J Phys Chem B 2004;108:8485–8. https://doi.org/10.1021/JP049271C.
[31] Lorenzón EN, Nobre TM, Caseli L, Cilli EM, da Hora GCA, Soares TA, et al. The "pre-assembled state" of magainin 2 lysine-linked dimer determines its enhanced antimicrobial activity. Colloids Surf B Biointerfaces 2018;167:432–40. https://doi.org/10.1016/J.COLSURFB.2018.04.034.
[32] Volinsky R, Kolusheva S, Berman A, Jelinek R. Microscopic visualization of alamethicin incorporation into model membrane monolayers. Langmuir 2004;20:11084–91. https://doi.org/10.1021/LA0477486.
[33] Golonka I, Puculek JE, Greber KE, Dryś A, Sawicki W, Musiał W. Evaluation of the effect of antibacterial peptides on model monolayers. Int J Mol Sci 2023;24:14861. https://doi.org/10.3390/IJMS241914861.
[34] Neville F, Cahuzac M, Nelson A, Gidalevitz D. The interaction of antimicrobial peptide LL-37 with artificial biomembranes:epifluorescence and impedance spectroscopy approach. J Phys Condens Matter 2004;16:S2413. https://doi.org/10.1088/0953-8984/16/26/014.
[35] Pastuszak K, Kowalczyk B, Tarasiuk J, Luchowski R, Gruszecki WI, Jurak M, et al. Insight into the mechanism of interactions between the LL-37 peptide and model membranes of legionella gormanii Bacteria. Int J Mol Sci 2023;24:12039. https://doi.org/10.3390/IJMS241512039/S1.
[36] Dannehl C, Brezesinski G, Möhwald H. Interactions of two fragments of the human antimicrobial peptide LL-37 with zwitterionic and anionic lipid monolayers. Zeitschrift Fur Physikalische Chemie 2015;229:1141–59. https://doi.org/10.1515/ZPCH-2014-0565/XML.
[37] Travkova OG, Andrä J, Möhwald H, Brezesinski G. Influence of arenicin on phase transitions and ordering of lipids in 2D model membranes. Langmuir 2013;29:12203–11. https://doi.org/10.1021/LA402340D.
[38] Travkova OG, Andrä J, MöHwald H, Brezesinski G. Conformational properties of arenicins: from the bulk to the air-water interface. ChemPhysChem 2010;11:3262–8. https://doi.org/10.1002/CPHC.201000472;ISSUE:ISSUE:DOI.
[39] Cavalli S, Handgraaf JW, Tellers EE, Popescu DC, Overhand M, Kjaer K, et al. Two-dimensional ordered β-sheet lipopeptide monolayers. J Am Chem Soc 2006;128:13959–66. https://doi.org/10.1021/JA065479V.
[40] Conde-Torres D, Calvelo M, Rovira C, Piñeiro Á, Garcia-Fandino R. Unlocking the specificity of antimicrobial peptide interactions for membrane-targeted therapies. Comput Struct Biotechnol J 2024;25:61–74. https://doi.org/10.1016/j.csbj.2024.04.022.
[41] Neville F, Ishitsuka Y, Hodges CS, Konovalov O, Waring AJ, Lehrer R, et al. Protegrin interaction with lipid monolayers: grazing incidence X-ray diffraction and X-ray reflectivity study. Soft Matter 2008;4:1665–74. https://doi.org/10.1039/B718295C.
[42] Gidalevitz D, Ishitsuka Y, Muresan AS, Konovalov O, Waring AJ, Lehrer RI, et al. Interaction of antimicrobial peptide protegrin with biomembranes. Proc Natl Acad Sci U S A 2003;100:6302–7. https://doi.org/10.1073/PNAS.0934731100;WEBSITE:WEBSITE:PNAS-SITE;WGROUP:STRING:PUBLICATION.
[43] Hädicke A, Schwieger C, Blume A. Cospreading of anionic phospholipids with peptides of the structure (KX)4K at the air–water interface: influence of lipid headgroup structure and hydrophobicity of the peptide on monolayer behavior. Langmuir 2017;33:12204–17. https://doi.org/10.1021/ACS.LANGMUIR.7B02255.
[44] Bertrand B, Garduño-Juárez R, Munoz-Garay C. Estimation of pore dimensions in lipid membranes induced by peptides and other biomolecules: a review. Biochim Biophys Acta 1863;2021:183551. https://doi.org/10.1016/J.BBAMEM.2021.183551.

[45] Erbe A, Kerth A, Dathe M, Blume A. Interactions of KLA amphipathic model peptides with lipid monolayers. ChemBioChem 2009;10:2884–92. https://doi.org/10.1002/CBIC.200900444;WEBSITE:WEBSITE:CHEMISTRY-EUROPE;REQUESTEDJOURNAL:JOURNAL:14397633;WGROUP:STRING:PUBLICATION.
[46] Bringezu F, Majerowicz M, Maltseva E, Wen S, Brezesinski G, Waring AJ. Penetration of the antimicrobial peptide dicynthaurin into phospholipid monolayers at the liquid–air interface. ChemBioChem 2007;8:1038–47. https://doi.org/10.1002/CBIC.200600503.
[47] Arouri A, Kerth A, Dathe M, Blume A. The binding of an amphipathic peptide to lipid monolayers at the air/water Interface is modulated by the lipid headgroup structure. Langmuir 2011;27:2811–8. https://doi.org/10.1021/LA104887S.
[48] Wang G. Database resources dedicated to antimicrobial peptides. In: Antimicrobial resistance and food safety: methods and techniques; 2015. p. 365–84. https://doi.org/10.1016/B978-0-12-801214-7.00018-1.
[49] Zhang K, Teng D, Mao R, Yang N, Hao Y, Wang J. Thinking on the construction of antimicrobial peptide databases: powerful tools for the molecular design and screening. Int J Mol Sci 2023;24:3134. https://doi.org/10.3390/IJMS24043134.
[50] Lin C, Xiong S, Cui F, Zhang Z, Shi H, Wei L. Deep learning in antimicrobial peptide prediction. J Chem Inf Model 2025;65:7373–92. https://doi.org/10.1021/ACS.JCIM.5C00530.
[51] Zhou X, Liu G, Cao S, Lv J. Deep learning for antimicrobial peptides: computational models and databases. J Chem Inf Model 2025;65:1708–17. https://doi.org/10.1021/ACS.JCIM.5C00006.
[52] Szymczak P, Zarzecki W, Wang J, Duan Y, Wang J, Coelho LP, et al. AI-driven antimicrobial peptide discovery: mining and generation. Acc Chem Res 2025;58:1831–46. https://doi.org/10.1021/ACS.ACCOUNTS.0C00594.
[53] Wang G, Li X, Wang Z. APD3: the antimicrobial peptide database as a tool for research and education. Nucleic Acids Res 2016;44:D1087–93. https://doi.org/10.1093/NAR/GKV1278.
[54] Wang G. The antimicrobial peptide database is 20 years old: recent developments and future directions. Protein Sci 2023;32:e4778. https://doi.org/10.1002/PRO.4778;CTYPE:STRING:JOURNAL.
[55] Shi G, Kang X, Dong F, Liu Y, Zhu N, Hu Y, et al. DRAMP 3.0: an enhanced comprehensive data repository of antimicrobial peptides. Nucleic Acids Res 2022;50:D488–96. https://doi.org/10.1093/NAR/GKAB651.
[56] Gawde U, Chakraborty S, Waghu FH, Barai RS, Khanderkar A, Indraguru R, et al. CAMPR4: a database of natural and synthetic antimicrobial peptides. Nucleic Acids Res 2023;51:D377–83. https://doi.org/10.1093/NAR/GKAC933.
[57] Jhong JH, Chi YH, Li WC, Lin TH, Huang KY, Lee TY. dbAMP: an integrated resource for exploring antimicrobial peptides with functional activities and physicochemical properties on transcriptome and proteome data. Nucleic Acids Res 2019;47:D285–97. https://doi.org/10.1093/NAR/GKY1030.
[58] Pirtskhalava M, Gabrielian A, Cruz P, Griggs HL, Squires RB, Hurt DE, et al. DBAASP v.2: an enhanced database of structure and antimicrobial/cytotoxic activity of natural and synthetic peptides. Nucleic Acids Res 2016;44:D1104–12. https://doi.org/10.1093/NAR/GKV1174.
[59] Ravichandran S, Avatapalli SS, Narasimhan Y, Kaushik KS, Yennamalli RM. "Targeting" the search: an upgraded structural and functional repository of antimicrobial peptides for biofilm studies (B-AMP v2.0) with a focus on biofilm protein targets. Front Cell Infect Microbiol 2022;12:1020391. https://doi.org/10.3389/FCIMB.2022.1020391/BIBTEX.
[60] Ramos-Martín F, Annaval T, Buchoux S, Sarazin C, D'Amelio N. ADAPTABLE: a comprehensive web platform of antimicrobial peptides tailored to the user's research. Life Sci Alliance 2019;2. https://doi.org/10.26508/LSA.201900512.
[61] Di Luca M, Maccari G, Maisetta G, Batoni G. BaAMPs: the database of biofilm-active antimicrobial peptides. Biofouling 2015;31:193–9. https://doi.org/10.1080/08927014.2015.1021340.
[62] Zhao X, Wu H, Lu H, Li G, Huang Q. LAMP: a database linking antimicrobial peptides. PloS One 2013;8:e66557. https://doi.org/10.1371/JOURNAL.PONE.0066557.
[63] Piotto SP, Sessa L, Concilio S, Iannelli P. YADAMP: yet another database of antimicrobial peptides. Int J Antimicrob Agents 2012;39:346–51. https://doi.org/10.1016/J.IJANTIMICAG.2011.12.003.
[64] Brahmachary M, Krishnan SPT, Koh JLY, Khan AM, Seah SH, Tan TW, et al. ANTIMIC: a database of antimicrobial sequences. Nucleic Acids Res 2004;32:D586–9. https://doi.org/10.1093/NAR/GKH032.
[65] Fjell CD, Hancock REW, Cherkasov A. AMPer: a database and an automated discovery tool for antimicrobial peptides. Bioinformatics 2007;23:1148–55. https://doi.org/10.1093/BIOINFORMATICS/BTM068.
[66] Li Y, Chen Z. RAPD: a database of recombinantly-produced antimicrobial peptides. FEMS Microbiol Lett 2008;289:126–9. https://doi.org/10.1111/J.1574-6968.2008.01357.X.
[67] Heimburg T. The excitable fluid mosaic. Biochim Biophys Acta 1865;2023:184104. https://doi.org/10.1016/J.BBAMEM.2022.184104.
[68] Aimo L, Liechti R, Hyka-Nouspikel N, Niknejad A, Gleizes A, Götz L, et al. The SwissLipids knowledgebase for lipid biology. Bioinformatics 2015;31:2860–6. https://doi.org/10.1093/BIOINFORMATICS/BTV285.
[69] Conroy MJ, Andrews RM, Andrews S, Cockayne L, Dennis EA, Fahy E, et al. LIPID MAPS: update to databases and tools for the lipidomics community. Nucleic Acids Res 2024;52:D1677–82. https://doi.org/10.1093/NAR/GKAD896.
[70] Symons JL, Cho KJ, Chang JT, Du G, Waxham MN, Hancock JF, et al. Lipidomic atlas of mammalian cell membranes reveals hierarchical variation induced by culture conditions, subcellular membranes, and cell lineages. Soft Matter 2021;17:288–97. https://doi.org/10.1039/D0SM00404A.
[71] Das S, Jain R, Banerjee KK, Chattopadhyay K, Karmakar S. Cholesterol-driven modulation of membrane-membrane interactions by an antimicrobial peptide, NK-2, in phospholipid vesicles. Biochem Biophys Res Commun 2024;741:151021. https://doi.org/10.1016/J.BBRC.2024.151021.
[72] Skowronska-Krawczyk D, Budin I. Aging membranes: unexplored functions for lipids in the lifespan of the central nervous system. Exp Gerontol 2020;131:110817. https://doi.org/10.1016/J.EXGER.2019.110817.
[73] Sasaki N, Toyoda M, Ishiwata T. Gangliosides as signaling regulators in cancer. Int J Mol Sci 2021;22:5076. https://doi.org/10.3390/IJMS22105076.
[74] Iltis C, Moskalevska I, Debiesse A, Seguin L, Fissoun C, Cervera L, et al. A ganglioside-based immune checkpoint enables senescent cells to evade immunosurveillance during aging. Nat Aging 2024;5(2):219–36. https://doi.org/10.1038/s43587-024-00776-z.
[75] Ahyayauch H, Masserini ME, Alonso A, Goñi FM. Understanding aβ peptide binding to lipid membranes: a biophysical perspective. Int J Mol Sci 2024;25:6401. https://doi.org/10.3390/IJMS25126401.
[76] Chakraborty S, Doktorova M, Molugu TR, Heberle FA, Scott HL, Dzikovski B, et al. How cholesterol stiffens unsaturated lipid membranes. Proc Natl Acad Sci U S A 2020;117:21896–905. https://doi.org/10.1073/PNAS.2004807117;WGROUP:STRING:PUBLICATION.
[77] Bramkamp M. Fluidity is the way to life: lipid phase separation in bacterial membranes. EMBO J 2022;41. https://doi.org/10.15252/EMBJ.2022110737;REQUESTEDJOURNAL:JOURNAL:14602075;PAGEGROUP:STRING:PUBLICATION.
[78] Brockman H. Lipid monolayers: why use half a membrane to characterize protein-membrane interactions? Curr Opin Struct Biol 1999;9:438–43. https://doi.org/10.1016/S0959-440X(99)80061-X.
[79] Dynarowicz-Latka P, Wnętrzak A, Chachaj-Brekiesz A. Advantages of the classical thermodynamic analysis of single - and multi-component Langmuir monolayers from molecules of biomedical importance - theory and applications. J R Soc Interface 2024;21. https://doi.org/10.1098/RSIF.2023.0559;SUBPAGE:STRING:FULL.
[80] Volinsky R, Kolusheva S, Berman A, Jelinek R. Investigations of antimicrobial peptides in planar film systems. Biochim Biophys Acta 2006;1758:1393–407. https://doi.org/10.1016/J.BBAMEM.2006.03.002.
[81] Redondo-Gómez C, Parreira P, Martins MCL, Azevedo HS. Peptide-based self-assembled monolayers (SAMs): what peptides can do for SAMs and vice versa. Chem Soc Rev 2024;53:3714–73. https://doi.org/10.1039/D3CS00921A.
[82] Xu Z, Brauner JW, Flach CR, Mendelsohn R. Orientation of peptides in aqueous monolayer films. infrared reflection−absorption spectroscopy studies of a synthetic amphipathic β-sheet. Langmuir 2004;20:3730–3. https://doi.org/10.1021/LA0304316.
[83] Di Napoli B, Mazzuca C, Conflitti P, Venanzi M, Palleschi A. Behavior of a peptide during a langmuir–blodgett compression isotherm: a molecular dynamics simulation study. J Phys Chem C 2017;122:515–21. https://doi.org/10.1021/ACS.JPCC.7B09850.
[84] Neville F, Ivankin A, Konovalov O, Gidalevitz D. A comparative study on the interactions of SMAP-29 with lipid monolayers. Biochim Biophys Acta 2010;1798:851–60. https://doi.org/10.1016/J.BBAMEM.2009.09.017.
[85] Alvares DS, Viegas TG, Ruggiero Neto J. Lipid-packing perturbation of model membranes by pH-responsive antimicrobial peptides. Biophys Rev 2017;9:669–82. https://doi.org/10.1007/S12551-017-0296-0/FIGURES/3.
[86] Pastuszak K, Jurak M, Kowalczyk B, Tarasiuk J, Wiącek AE, Palusińska-Szysz M. Susceptibility of legionella gormanii membrane-derived phospholipids to the peptide action of antimicrobial LL-37—Langmuir monolayer studies. Molecules 2024;29:1522. https://doi.org/10.3390/MOLECULES29071522/S1.
[87] Knyght I, Clifton L, Saaka Y, Lawrence MJ, Barlow DJ. Interaction of the antimicrobial peptides Rhesus θ-defensin and porcine Protegrin-1 with anionic phospholipid monolayers. Langmuir 2016;32:7403–10. https://doi.org/10.1021/ACS.LANGMUIR.6B01688.
[88] Pastuszak K, Palusińska-Szysz M, Wiącek AE, Jurak M. Thermodynamic study on biomimetic *Legionella gormanii* bacterial membranes. Molecules 2024;29:4367. https://doi.org/10.3390/MOLECULES29184367.
[89] Hädicke A, Blume A. Binding of the cationic peptide (KL)4K to lipid monolayers at the air–water interface: effect of lipid headgroup charge, acyl chain length, and acyl chain saturation. J Phys Chem B 2016;120:3880–7. https://doi.org/10.1021/ACS.JPCB.6B01558.
[90] Pastuszak K, Kowalczyk B, Tarasiuk J, Jurak M, Palusińska-Szysz M. Influence of the antimicrobial LL-37 peptide on *Legionella dumoffii* phospholipids adsorbed at the air–liquid interface. Sustainability 2023;15:6670. https://doi.org/10.3390/SU15086670.
[91] Gochev GG, Campbell RA, Schneck E, Zawala J, Warszynski P. Exploring proteins at soft interfaces and in thin liquid films – from classical methods to advanced applications of reflectometry. Adv Colloid Interface Sci 2024;329:103187. https://doi.org/10.1016/J.CIS.2024.103187.
[92] Elderdfi M, Sikorski AF. Langmuir-monolayer methodologies for characterizing protein-lipid interactions. Chem Phys Lipids 2018;212:61–72. https://doi.org/10.1016/J.CHEMPHYSLIP.2018.01.008.
[93] Zuo YY, Chen R, Wang X, Yang J, Policova Z, Neumann AW. Phase transitions in dipalmitoylphosphatidylcholine monolayers. Langmuir 2016;32:8501–6. https://doi.org/10.1021/ACS.LANGMUIR.6B01482.
[94] Dervichian DG. Changes of phase and transformations of higher order in monolayers. J Chem Phys 1939;7:931–48. https://doi.org/10.1063/1.1750347.
[95] Harkins WD, Young TF, Boyd E. The thermodynamics of films: energy and entropy of extension and spreading of insoluble monolayers. J Chem Phys 1940;8:954–65. https://doi.org/10.1063/1.1750610.
[96] Gochev GG, Kovalchuk VI, Aksenenko EV, Fainerman VB, Miller R. B-Lactoglobulin adsorption layers at the water/air surface: 5. Adsorption isotherm

and equation of state revisited, impact of pH, colloids and interfaces5; 2021. p. 14. https://doi.org/10.3390/COLLOIDS5010014.
[97] Maget-Dana R. The monolayer technique: a potent tool for studying the interfacial properties of antimicrobial and membrane-lytic peptides and their interactions with lipid membranes. Biochim Biophys Acta Biomembr 1999;1462: 109–40. https://doi.org/10.1016/S0005-2736(99)00203-5.
[98] Caruso B, Ambroggio EE, Wilke N, Fidelio GD. The rheological properties of beta amyloid Langmuir monolayers: comparative studies with melittin peptide. Colloids Surf B Biointerfaces 2016;146:180–7. https://doi.org/10.1016/J.COLSURFB.2016.06.003.
[99] Zapolski R, Gasztych M, Jastrząb-Miśkiewicz B, Jankowska-Konsur A, Musiał W. The properties of the monolayers of sorbitan lipids as informative factors on the hydrophilic–lipophilic balance value of their mixtures, proposed for dermatological applications. Molecules 2025;30:1841. https://doi.org/10.3390/MOLECULES30081841.
[100] Ambroggio EE, Kim DH, Separovic F, Barrow CJ, Barnham KJ, Bagatolli LA, et al. Surface behavior and lipid interaction of Alzheimer β-amyloid peptide 1-42: a membrane-disrupting peptide. Biophys J 2005;88:2706–13. https://doi.org/10.1529/biophysj.104.055582.
[101] Pagano RE, Gershfeld NL. Physical chemistry of lipid films at the air-water interface. II. Binary lipid mixtures. Principles governing miscibility of lipids in surfaces. J Phys Chem 2002;76:1238–43. https://doi.org/10.1021/J100653A002.
[102] Frigini EN, Porasso RD, Beke-Somfai T, López Cascales JJ, Enriz RD, Pantano S. The mechanism of antimicrobial small-cationic peptides from coarse-grained simulations. J Chem Inf Model 2023;63:6877–89. https://doi.org/10.1021/ACS.JCIM.3C01348.
[103] Birdi KS, Gevod VS, Ksenzhek OS, Stenby E, Rasmussen KL. Equation of state for monomolecular films of melittin at air-water interface. Colloid Polym Sci 1983; 261:767–75. https://doi.org/10.1007/BF01410951/METRICS.
[104] Fainerman VB, Vollhardt D. Penetration of Langmuir monolayers by soluble amphiphilic molecules. Langmuir 1999;15:1784–90. https://doi.org/10.1021/LA9809271.
[105] Vollhardt D, Fainerman VB. Penetration of dissolved amphiphiles into two-dimensional aggregating lipid monolayers. Adv Colloid Interface Sci 2000;86: 103–51. https://doi.org/10.1016/S0001-8686(00)00034-8.
[106] Ivanov IB, Ananthapadmanabhan KP, Lips A. Adsorption and structure of the adsorbed layer of ionic surfactants. Adv Colloid Interface Sci 2006;123–126: 189–212. https://doi.org/10.1016/J.CIS.2006.05.020.
[107] Cuadros F, Mulero A, Morala L, Gómez-Serrano V. Isosteric heat for monolayer adsorption obtained from two-dimensional equations of state. Langmuir 2001;17: 1576–81. https://doi.org/10.1021/LA0014048.
[108] Campelo F, Arnarez C, Marrink SJ, Kozlov MM. Helfrich model of membrane bending: from Gibbs theory of liquid interfaces to membranes as thick anisotropic elastic layers. Adv Colloid Interface Sci 2014;208:25–33. https://doi.org/10.1016/J.CIS.2014.01.018.
[109] Tu ZC, Ou-Yang ZC. Recent theoretical advances in elasticity of membranes following Helfrich's spontaneous curvature model. Adv Colloid Interface Sci 2014;208:66–75. https://doi.org/10.1016/J.CIS.2014.01.008.
[110] Takahashi A, Yoshida A, Kawaguchi M. Test of scaling laws describing the concentration dependence of surface pressure of a polymer monolayer. Macromolecules 2002;15:1196–8. https://doi.org/10.1021/MA00232A047.
[111] Glandt ED, Myers AL, Fitts DD. Two-dimensional equations of state: a comparison with experiment. J Chem Phys 1979;70:4243–7. https://doi.org/10.1063/1.437997.
[112] Fainerman VB, Miller R. Equation of state for concentrated protein surface layers at the water/air Interface. Langmuir 1999;15:1812–6. https://doi.org/10.1021/LA981180H.
[113] Joos P. Approach for an equation of state for adsorbed protein surfaces. Biochim Biophys Acta 1975;375:1–9. https://doi.org/10.1016/0005-2736(75)90067-X.
[114] Toxvaerd S. The equation of state of dense fluid monolayers. J Chem Phys 1977; 67:2056–60. https://doi.org/10.1063/1.435089.
[115] Uraizee F, Narsimhan G. A surface equation of state for globular proteins at the air-water interface. J Colloid Interface Sci 1991;146:169–78. https://doi.org/10.1016/0021-9797(91)90014-Y.
[116] Rojewska M, Smułek W, Kaczorek E, Prochaska K. Langmuir monolayer techniques for the investigation of model bacterial membranes and antibiotic biodegradation mechanisms. Membranes (Basel) 2021;11. https://doi.org/10.3390/MEMBRANES11090707.
[117] Ciumac D, Gong H, Campbell RA, Campana M, Xu H, Lu JR. Structural elucidation upon binding of antimicrobial peptides into binary mixed lipid monolayers mimicking bacterial membranes. J Colloid Interface Sci 2021;598:193–205. https://doi.org/10.1016/J.JCIS.2021.04.037.
[118] Tyteca D, Schanck A, Dufrêne YF, Deleu M, Courtoy PJ, Tulkens PM, et al. The macrolide antibiotic azithromycin interacts with lipids and affects membrane organization and fluidity: studies on langmuir-blodgett monolayers, liposomes and J774 macrophages. J Membr Biol 2003;192(3):203–15. https://doi.org/10.1007/S00232-002-1076-7.
[119] Gong H, Hu X, Zhang L, Fa K, Liao M, Liu H, et al. How do antimicrobial peptides disrupt the lipopolysaccharide membrane leaflet of Gram-negative bacteria? J Colloid Interface Sci 2023;637:182–92. https://doi.org/10.1016/J.JCIS.2023.01.051.
[120] Golonka I, Łukasiewicz IW, Sebastiańczyk A, Greber KE, Sawicki W, Musiał W. The role of temperature and subphase components in shaping selected physicochemical properties of the phosphatidylinositol monolayer. Int J Mol Sci 2025;26:3472. https://doi.org/10.3390/IJMS26083472.
[121] Golonka I, Łukasiewicz IW, Sebastiańczyk A, Greber KE, Sawicki W, Musiał W. The influence of the amphiphilic properties of peptides on the phosphatidylinositol monolayer in the presence of ascorbic acid. Int J Mol Sci 2024;25:12484. https://doi.org/10.3390/IJMS252312484/S1.
[122] Gast A, Adamson T, Adamson A, Gast A, Adamson Arthur W, Alice P. Gast - physical chemistry of surfaces. https://www.wiley.com/en-us/Physical+Chemistry+of+Surfaces%2C+6th+Edition-p-9780471148739. [Accessed 26 November 2025].
[123] Ciutara CO, Barman S, Iasella S, Huang B, Zasadzinski JA. Dilatational and shear rheology of soluble and insoluble monolayers with a Langmuir trough. J Colloid Interface Sci 2023;629:125–35. https://doi.org/10.1016/J.JCIS.2022.08.051.
[124] Cicuta P, Terentjev EM. Viscoelasticity of a protein monolayer from anisotropic surface pressure measurements. Eur Phys J E 2005;16:147–58. https://doi.org/10.1140/EPJE/E2005-00016-Y.
[125] Sudjarwo WAA, Toca-Herrera JL. Surface rheological properties and microstructures of DPPC/POPC monolayers. Langmuir 2025;41:16128–38. https://doi.org/10.1021/ACS.LANGMUIR.5C01269.
[126] Jaroque GN, dos Santos AL, Sartorelli P, Caseli L. Surface chemistry of cytosporone-B incorporated in models for microbial biomembranes as Langmuir monolayers. Langmuir 2024. https://doi.org/10.1021/ACS.LANGMUIR.4C01575.
[127] Wang Q, Wei S, Wu J, Zou X, Sieggreen O, Liu Y, et al. Interfacial behaviors of antimicrobial peptide cecropin P1 immobilized on different self-assembled monolayers. J Phys Chem C 2015;119:22542–51. https://doi.org/10.1021/ACS.JPCC.5B06882.
[128] Li Y, Wei S, Wu J, Jasensky J, Xi C, Li H, et al. Effects of peptide immobilization sites on the structure and activity of surface-tethered antimicrobial peptides. J Phys Chem C 2015;119:7146–55. https://doi.org/10.1021/JP5125487.
[129] Han X, Zheng J, Lin F, Kuroda K, Chen Z. Interactions between surface-immobilized antimicrobial peptides and model bacterial cell membranes. Langmuir 2017;34:512–20. https://doi.org/10.1021/ACS.LANGMUIR.7B03411.
[130] S.H. North, C. So, K. Fears, C.R. Taitt, Chemoselective surface attachment of antimicrobial peptides and its effects on interfacial behavior, 9112 (2014) 136–143. doi: https://doi.org/10.1117/12.2053353.
[131] Ivanov IE, Morrison AE, Cobb JE, Fahey CA, Camesano TA. Creating antibacterial surfaces with the peptide Chrysophsin-1. ACS Appl Mater Interfaces 2012;4: 5891–7. https://doi.org/10.1021/AM301530A.
[132] Xiao M, Jasensky J, Gerszberg J, Chen J, Tian J, Lin T, et al. Chemically immobilized antimicrobial peptide on polymer and self-assembled monolayer substrates. Langmuir 2018;34:12889–96. https://doi.org/10.1021/ACS.LANGMUIR.8B02377.
[133] Khmelinskaia A, Mücksch J, Conci F, Chwastek G, Schwille P. FCS analysis of protein mobility on lipid monolayers. Biophys J 2018;114:2444–54. https://doi.org/10.1016/j.bpj.2018.02.031.
[134] Zorila B, Necula G, Janosi L, Turcu I, Bacalum M, Radu M. Interaction of arginine and tryptophan-rich short antimicrobial peptides with membrane models: a combined fluorescence, simulations, and theoretical approach. J Chem Inf Model 2025;65:3723–36. https://doi.org/10.1021/ACS.JCIM.5C00139.
[135] Haefele T, Kita-Tokarczyk K, Meier W. Phase behavior of mixed Langmuir monolayers from amphiphilic block copolymers and an antimicrobial peptide. Langmuir 2005;22:1164–72. https://doi.org/10.1021/LA0524216.
[136] Burdach K, Tymecka D, Urban A, Lasek R, Bartosik D, Sek S. Interactions of linear analogues of battacin with negatively charged lipid membranes. Membranes 2021;11:192. https://doi.org/10.3390/MEMBRANES11030192.
[137] Neville F, Cahuzac M, Konovalov O, Ishitsuka Y, Lee KYC, Kuzmenko I, et al. Lipid headgroup discrimination by antimicrobial peptide LL-37: insight into mechanism of action. Biophys J 2006;90:1275–87. https://doi.org/10.1529/biophysj.105.067595.
[138] Majerowicz M, Waring AJ, Wen S, Bringezu F. Interaction of the antimicrobial peptide dicynthaurin with membrane phospholipids at the air−liquid Interface. J Phys Chem B 2007;111:3813–21. https://doi.org/10.1021/JP0672398.
[139] Alexander PJ, Oyama LB, Olleik H, Godoy Santos F, O'Brien S, Cookson A, et al. Microbiome-derived antimicrobial peptides show therapeutic activity against the critically important priority pathogen, *Acinetobacter baumannii*. Npj Biofilms Microbiom 2024;10:92. https://doi.org/10.1038/s41522-024-00560-2.
[140] Freire RVM, Pillco-Valencia Y, da Hora GCA, Ramstedt M, Sandblad L, Soares TA, et al. Antimicrobial peptide induced colloidal transformations in bacteria-mimetic vesicles: combining in silico tools and experimental methods. J Colloid Interface Sci 2021;596:352–63. https://doi.org/10.1016/J.JCIS.2021.03.060.
[141] Hartmann M, Berditsch M, Hawecker J, Ardakani MF, Gerthsen D, Ulrich AS. Damage of the bacterial cell envelope by antimicrobial peptides gramicidin S and PGLa as revealed by transmission and scanning electron microscopy. Antimicrob Agents Chemother 2010;54:3132–42. https://doi.org/10.1128/AAC.00124-10;CTYPE:STRING:JOURNAL.
[142] Izadi S, Anandakrishnan R, Onufriev AV. Building water models: a different approach. J Phys Chem Lett 2014;5:3863–71. https://doi.org/10.1021/JZ501780A.
[143] Klauda JB, Venable RM, Freites JA, O'Connor JW, Tobias DJ, Mondragon-Ramirez C, et al. Update of the CHARMM all-atom additive force field for lipids: validation on six lipid types. J Phys Chem B 2010;114:7830–43. https://doi.org/10.1021/JP101759Q.
[144] Tempra C, Ollila OHS, Javanainen M. Accurate simulations of lipid monolayers require a water model with correct surface tension. J Chem Theory Comput 2022; 18:1862–9. https://doi.org/10.1021/ACS.JCTC.1C00951.

[145] McCluskey AR, Grant J, Smith AJ, Rawle JL, Barlow DJ, Lawrence MJ, et al. Assessing molecular simulation for the analysis of lipid monolayer reflectometry. J Phys Commun 2019;3:075001. https://doi.org/10.1088/2399-6528/AB12A9.
[146] Javanainen M, Lamberg A, Cwiklik L, Vattulainen I, Ollila OHS. Atomistic model for nearly quantitative simulations of Langmuir monolayers. Langmuir 2017;34:2565–72. https://doi.org/10.1021/ACS.LANGMUIR.7B02855.
[147] Bowers SR, Lockhart C, Klimov DK. Replica exchange with hybrid tempering efficiently samples PGLa peptide binding to anionic bilayer. J Chem Theory Comput 2023;19:6532–50. https://doi.org/10.1021/ACS.JCTC.3C00787.
[148] Corey RA, Vickery ON, Sansom MSP, Stansfeld PJ. Insights into membrane protein–lipid interactions from free energy calculations. J Chem Theory Comput 2019;15:5727–36. https://doi.org/10.1021/ACS.JCTC.9B00548.
[149] Chen CH, Wiedman G, Khan A, Ulmschneider MB. Absorption and folding of melittin onto lipid bilayer membranes via unbiased atomic detail microsecond molecular dynamics simulation. Biochim Biophys Acta 2014;1838:2243–9. https://doi.org/10.1016/J.BBAMEM.2014.04.012.
[150] Wang Y, Chen CH, Hu D, Ulmschneider MB, Ulmschneider JP. Spontaneous formation of structurally diverse membrane channel architectures from a single antimicrobial peptide. Nat Commun 2016;7(1):13535. https://doi.org/10.1038/ncomms13535.
[151] Otero-Mato JM, Montes-Campos H, Calvelo M, García-Fandino R, Gallego LJ, Pineiro Á, et al. GADDLE maps: general algorithm for discrete object deformations based on local exchange maps. J Chem Theory Comput 2018;14:466–78. https://doi.org/10.1021/ACS.JCTC.7B00861.
[152] Conchillo-Solé O, de Groot NS, Avilés FX, Vendrell J, Daura X, Ventura S. AGGRESCAN: a server for the prediction and evaluation. BMC Bioinformatics 2007;8(1):65. https://doi.org/10.1186/1471-2105-8-65.
[153] Fernandez-Escamilla AM, Rousseau F, Schymkowitz J, Serrano L. Prediction of sequence-dependent and mutational effects on the aggregation of peptides and proteins. Nat Biotechno 2004;22(10):1302–6. https://doi.org/10.1038/nbt1012.
[154] Maleš M, Zoranić L. Simulation study of the effect of antimicrobial peptide associations on the mechanism of action with bacterial and eukaryotic membranes. Membranes (Basel) 2022;12:891. https://doi.org/10.3390/MEMBRANES12090891/S1.
[155] Parton DL, Akhmatskaya EV, Sansom MSP. Multiscale simulations of the antimicrobial peptide maculatin 1.1: water permeation through disordered aggregates. J Phys Chem B 2012;116:8485–93. https://doi.org/10.1021/JP212358Y.
[156] Duncan SL, Larson RG. Folding of lipid monolayers containing lung surfactant proteins SP-B1–25 and SP-C studied via coarse-grained molecular dynamics simulations. Biochim Biophys Acta 2010;1798:1632–50. https://doi.org/10.1016/J.BBAMEM.2010.04.006.
[157] Santer M. New insights into lipid monolayers from coarse-grained simulation techniques. Biophys J 2014;107:1038–9. https://doi.org/10.1016/j.bpj.2014.07.030.
[158] Feng S, Park S, Choi YK, Im W. CHARMM-GUI membrane builder: past, current, and future developments and applications. J Chem Theory Comput 2023;19:2161–85. https://doi.org/10.1021/ACS.JCTC.2C01246.
[159] Jo S, Kim T, Iyer VG, Im W. CHARMM-GUI: a web-based graphical user interface for CHARMM. J Comput Chem 2008;29:1859–65. https://doi.org/10.1002/JCC.20945;JOURNAL:JOURNAL:1096987X;WGROUP:STRING:PUBLICATION.
[160] Abraham MJ, Murtola T, Schulz R, Páll S, Smith JC, Hess B, et al. GROMACS: high performance molecular simulations through multi-level parallelism from laptops to supercomputers. SoftwareX 2015;1–2:19–25. https://doi.org/10.1016/J.SOFTX.2015.06.001.
[161] Thompson AP, Aktulga HM, Berger R, Bolintineanu DS, Brown WM, Crozier PS, et al. LAMMPS - a flexible simulation tool for particle-based materials modeling at the atomic, meso, and continuum scales. Comput Phys Commun 2022;271:108171. https://doi.org/10.1016/J.CPC.2021.108171.
[162] Case DA, Cheatham TE, Darden T, Gohlke H, Luo R, Merz KM, et al. The Amber biomolecular simulation programs. J Comput Chem 2005;26:1668–88. https://doi.org/10.1002/JCC.20290;JOURNAL:JOURNAL:1096987X;WGROUP:STRING:PUBLICATION.
[163] Eastman P, Pande VS. OpenMM: a hardware-independent framework for molecular simulations. Comput Sci Eng 2010;12:34–9. https://doi.org/10.1109/MCSE.2010.27.
[164] Brooks BR, Brooks CL, Mackerell AD, Nilsson L, Petrella RJ, Roux B, et al. CHARMM: the biomolecular simulation program. J Comput Chem 2009;30:1545–614. https://doi.org/10.1002/JCC.21287;JOURNAL:JOURNAL:1096987X;WGROUP:STRING:PUBLICATION.
[165] Phillips JC, Hardy DJ, Maia JDC, Stone JE, Ribeiro JV, Bernardi RC, et al. Scalable molecular dynamics on CPU and GPU architectures with NAMD. J Chem Phys 2020;153. https://doi.org/10.1063/5.0014475/1064953.
[166] Gowers RJ, Linke M, Barnoud J, Reddy TJE, Melo MN, Seyler SL, et al. MDAnalysis: a Python package for the rapid analysis of molecular dynamics simulations. SciPy 2016;2016:98–105. https://doi.org/10.25080/MAJORA-629E541A-00E.
[167] Smith P, Lorenz CD. LiPyphilic: a Python toolkit for the analysis of lipid membrane simulations. J Chem Theory Comput 2021;17:5907–19. https://doi.org/10.1021/ACS.JCTC.1C00447.
[168] Sega M, Hantal G, Fábián B, Jedlovszky P. Pytim: a python package for the interfacial analysis of molecular simulations. J Comput Chem 2018;39:2118–25. https://doi.org/10.1002/JCC.25384;ISSUE:ISSUE:DOI.
[169] Santos DES, Pontes FJS, Lins RD, Coutinho K, Soares TA. SuAVE: a tool for analyzing curvature-dependent properties in chemical interfaces. J Chem Inf Model 2019;60:473–84. https://doi.org/10.1021/ACS.JCIM.9B00569.
[170] Domański J, Stansfeld PJ, Sansom MSP, Beckstein O. Lipidbook: a public repository for force-field parameters used in membrane simulations. J Membr Biol 2010;236(3):255–8. https://doi.org/10.1007/S00232-010-9296-8.
[171] A.M. Kiirikki, H.S. Antila, L.S. Bort, P. Buslaev, F. Favela-Rosales, T.M. Ferreira, P. F.J. Fuchs, R. Garcia-Fandino, I. Gushchin, B. Kav, N. Kučerka, P. Kula, M. Kurki, A. Kuzmin, A. Lalitha, F. Lolicato, J.J. Madsen, M.S. Miettinen, C. Mingham, L. Monticelli, R. Nencini, A.M. Nesterenko, T.J. Piggot, Á. Piñeiro, N. Reuter, S. Samantray, F. Suárez-Lestón, R. Talandashti, O.H.S. Ollila, Overlay databank unlocks data-driven analyses of biomolecules for all, Nat Commun 2024 15:1 (2024) 1136. doi: https://doi.org/10.1038/s41467-024-45189-z.
[172] Biriukov D, Vácha R. Pathways to a shiny future: building the foundation for computational physical chemistry and biophysics in 2050. ACS Phys Chem Au 2024;4:302–13. https://doi.org/10.1021/ACSPHYSCHEMAU.4C00003.
[173] Das P, Sercu T, Wadhawan K, Padhi I, Gehrmann S, Cipcigan F, et al. Accelerated antimicrobial discovery via deep generative models and molecular dynamics simulations. Nat Biomed Eng 2021;5(6):613–23. https://doi.org/10.1038/s41551-021-00689-x.
[174] Brizuela CA, Liu G, Stokes JM, de la Fuente-Nunez C. AI methods for antimicrobial peptides: progress and challenges. J Microbial Biotechnol 2025;18:e70072. https://doi.org/10.1111/1751-7915.70072;PAGE:STRING:ARTICLE/CHAPTER.
[175] Conde-Torres D, Mussa-Juane M, Faílde D, Gómez A, García-Fandiño R, Piñeiro Á. Classical simulations on quantum computers: interface-driven peptide folding on simulated membrane surfaces. Comput Biol Med 2024;182:109157. https://doi.org/10.1016/J.COMPBIOMED.2024.109157.
[176] Wang G, Mishra B, Epand RF, Epand RM. High-quality 3D structures shine light on antibacterial, anti-biofilm and antiviral activities of human cathelicidin LL-37 and its fragments. Biochim Biophys Acta 2014;1838:2160–72. https://doi.org/10.1016/J.BBAMEM.2014.01.016.
[177] Golonka I, Greber KE, Szyja BM, Petrus PP, Pucułek JE, Musiał W. Effect of newly synthesized structures of peptides on the stability of the monolayers formed. Int J Mol Sci 2023;24:4318. https://doi.org/10.3390/IJMS24054318.